JOURNAL OF PETROLOGY | VOLUME 47 | NUMBER 1 | PAGES 119–144 | 2006 | doi:10.1093/petrology/egi070

Petrogenesis of Adakitic Porphyries in an Extensional Tectonic Setting, Dexing, South China: Implications for the Genesis of Porphyry Copper Mineralization

QIANG WANG[1]*, JI-FENG XU[1], PING JIAN[2], ZHI-WEI BAO[1], ZHEN-HUAN ZHAO[1], CHAO-FENG LI[3], XIAO-LIN XIONG[1] AND JIN-LONG MA[1]

[1]KEY LABORATORY OF ISOTOPE GEOCHRONOLOGY AND GEOCHEMISTRY, GUANGZHOU INSTITUTE OF GEOCHEMISTRY, CHINESE ACADEMY OF SCIENCES, GUANGZHOU 510640, P.R. CHINA

[2]CHINESE ACADEMY OF GEOLOGICAL SCIENCE, 26 BEIWANZHUANG ROAD, BEIJING 100037, P.R. CHINA

[3]INSTITUTE OF GEOLOGY AND GEOPHYSICS, CHINESE ACADEMY OF SCIENCES, BEIJING 100029, P.R. CHINA

RECEIVED APRIL 8, 2004; ACCEPTED JULY 6, 2005
ADVANCE ACCESS PUBLICATION AUGUST 17, 2005

The Dexing adakitic porphyries (quartz diorite–granodiorite porphyries), associated with giant porphyry Cu deposits, are located in the interior of a continent (South China). They exhibit relatively high MgO, Cr, Ni and Sr contents, high La/Yb and Sr/Y ratios, but low Yb and Y contents, similar to adakites produced by slab melting associated with subduction. However, they are characterized by bulk Earth-like Nd–Sr isotope compositions ($\varepsilon_{Nd}(t) = -1{\cdot}14$ to $+1{\cdot}80$ and $(^{87}Sr/^{86}Sr)_i = 0{\cdot}7044 - 0{\cdot}7047$), and high Th (12·6–27·2 ppm) contents and Th/Ce (0·19–0·94) ratios, which are different from those of Cenozoic slab-derived adakites. Sensitive High-Resolution Ion Microprobe (SHRIMP) geochronology studies of zircons reveal that the Dexing adakitic porphyries have a crystallization age of 171 ± 3 Ma. This age is contemporaneous with Middle Jurassic extension within the Shi-Han rift zone, and within-plate magmatism elsewhere in South China, indicating that the Dexing adakitic porphyries were probably formed in an extensional tectonic regime in the interior of the continent rather than in an arc setting. Their high Th contents and Th/Ce ratios, and Middle Jurassic age, argue against an origin from a Neoproterozoic (~1000 Ma) stalled slab in the mantle. Taking into account available data for the regional metamorphic–magmatic rocks, and the present-day crustal thickness (~31 km) in the area, we suggest that the Dexing adakitic porphyries were most probably generated by partial melting of delaminated lower crust, which was possibly triggered by upwelling of the asthenospheric mantle due to the activity of the Shi-Hang rift zone. Moreover, the Dexing adakitic magmas must have interacted with the surrounding mantle peridotite during their ascent, which elevated not only their MgO, Cr and Ni contents, but also the oxygen fugacity (fO_2) of the mantle. The high fO_2 could have induced oxidation of metallic sulfides in the mantle and mobilization of chalcophile elements, which are required to produce associated Cu mineralization. Therefore, the Cu metallogenesis associated with the Dexing adakitic porphyries is probably related to partial melting of delaminated lower crust, similar to the metallogenesis accompanying slab melting.

KEY WORDS: *adakite; lower crust; delamination; porphyry copper deposit, South China*

INTRODUCTION

Defant & Drummond (1990) proposed that partial melting of a subducting oceanic slab at sufficient depths for garnet to be stable within the residual assemblage (i.e. residues of garnet-amphibolite, amphibole-bearing eclogite and/or eclogite) can generate andesitic, dacitic and rhyolitic rocks with rather unusual geochemical characteristics (e.g. high Sr, Sr/Y and La/Yb values and low Y

*Corresponding author. Telephone: + 86-20-8529 0277. Fax: +86-20-8529 0130. E-mail: wqiang@gig.ac.cn

and Yb contents). They named these rocks adakites, following the terminology of Kay (1978), who was the first to attribute a slab-melting scenario for similar rocks at Adak Island in the Aleutian arc. Since then, adakites have frequently been suggested as possible examples of partial melts of subducted oceanic crust (e.g. Kay *et al.*, 1993; Stern & Kilian, 1996; Gutscher *et al.*, 2000; Hollings & Kerrich, 2000; Sajona *et al.*, 2000; Wyman *et al.*, 2000; Aguillón-Robles *et al.*, 2001; Bourdon *et al.*, 2002; Polt & Kerrich, 2002; Martin *et al.*, 2005). Recently, it has also been recognized that adakites are often associated with Cu–Au mineralization (Thiéblemont *et al.*, 1997; Oyarzún *et al.*, 2001; Defant *et al.*, 2002; Mungall, 2002; Qu *et al.*, 2004), suggesting a genetic relationship between slab melting and Cu–Au mineralization.

On the other hand, it has also been suggested that some adakitic rocks may be derived by partial melting of thickened lower crust (e.g. Atherton & Petford, 1993; Muir *et al.*, 1995; Petford & Atherton, 1996; Johnson *et al.*, 1997; Arculus *et al.*, 1999; Zhang *et al.*, 2001; Chung *et al.*, 2003; Xiong *et al.*, 2003; Wang *et al.*, 2005) or delaminated mafic lower crust (e.g. Kay & Kay, 1993; Defant *et al.*, 2002; Xu *et al.*, 2002; Gao *et al.*, 2004; Wang *et al.*, 2004*a*, 2004*b*), as well as by assimilation and fractional crystallization (AFC) processes from parental basaltic magmas (e.g. Castillo *et al.*, 1999). It should be noted that most Cenozoic adakites occur in arc settings (Defant & Drummond, 1990; Defant *et al.*, 2002). Thus, it is very difficult to distinguish lower crust-derived adakitic rocks in arc settings from subducting slab-derived adakites that may be contaminated by crustal material during their ascent to the surface (e.g. Gutscher *et al.*, 2000).

Mungall (2002) concluded that only slab-derived melts, or supercritical fluids with high oxygen fugacity (fO_2) had the potential to generate associated epithermal and porphyry Cu–Au deposits, as adakitic magmas derived due to basaltic or gabbroic lower crustal melting should retain the low fO_2 of their source. Nevertheless, it has been recently recognized that some Cenozoic adakitic rocks derived by lower crustal melting are also associated with porphyry Cu–Au deposits (e.g. Richards, 2002; Bissig *et al.*, 2003; Hou *et al.*, 2004). Accordingly, the relationship between adakites and associated porphyry Cu–Au mineralization needs to be further re-examined or clarified.

In southern China, the famous Dexing large-scale porphyry copper deposits are closely associated with late Mesozoic adakitic porphyries (Wang *et al.*, 2003*a*). Owing to extensive hydrothermal alteration, the available Rb–Sr and K–Ar ages of the porphyries are unreliable and fall in a wide range from 193 to 112 Ma (early Jurassic–Cretaceous) (Zhu *et al.*, 1983; Hua & Dong, 1984; Rui *et al.*, 1984; Zhu *et al.*, 1990; Chen & Jahn, 1998; Jin *et al.*, 2002). However, in this study, new Sensitive High-Resolution Ion Microprobe (SHRIMP) zircon geochronology data show that the porphyries were intruded in the Middle Jurassic (171 ± 3 Ma), synchronous with an extensional tectonic event rather than in a compressional tectonic regime (Gilder *et al.*, 1996; Zhao *et al.*, 2001; Li *et al.*, 2003, 2004; Wang *et al.*, 2003*b*, 2004*c*). The occurrence of adakitic rocks and associated large-scale copper deposits in an extensional tectonic setting provides a good opportunity for understanding the genetic relationship between adakitic magmatism and porphyry Cu–Au mineralization. In this paper, we present a detailed account of the geochronology, petrology and geochemistry of the Middle Jurassic Dexing adakitic porphyries and address the petrogenesis and the relationship between these adakitic rocks and their associated Cu mineralization.

GEOLOGICAL BACKGROUND

South China consists of two cratonic lithospheric blocks—the Yangtze Block and the Cathaysia Block—separated by the Jiangshao (Jiangshan–Shaoxing) fault zone (Fig. 1a and b; Chen & Jahn, 1998), which is considered to be a major Neoproterozoic tectonic suture zone (Zhou & Zhu, 1993; Li *et al.*, 1997, 2002*a*; Zhou *et al.*, 2002). Geological, petrological and geochronological studies have confirmed that the Yangtze and Cathaysia Blocks have been a single terrane since the Neoproterozoic collision between the two blocks (Chen *et al.*, 1991; Zhou & Zhu, 1993; Li *et al.*, 1997, 2002*a*; Chen & Jahn, 1998; Zhou *et al.*, 2002). The crust of the Yangtze Block is mainly composed of Proterozoic metamorphic rocks which contain the Banxi–Sibao Group (1800 Ma) in NW Yangtze Block, the Shuangqiaoshan–Shangxi Group (1400 Ma) in SE Yangtze Block, and the Shuangxiwu Group (~1000–875 Ma), which occurs near the boundary between the Yangtze Block and Cathaysia Block (Chen & Jahn, 1998). Most of the rocks of the Shuangxiwu Group (southeast of the Yangtze Block) were formed in an arc setting in the Neoproterozoic; they include metamorphosed arc volcanic rocks (978–875 Ma) and metasediments (Zhou & Zhu, 1993; Li *et al.*, 2002*a*; Zhou *et al.*, 2002). The formations overlying the Proterozoic metamorphic basement in the Yangtze Block are sedimentary strata of Neoproterozoic (Sinian) to Triassic age (800–200 Ma). It is commonly considered that South China experienced a Triassic compressional event (e.g. Chen, 1999; Li *et al.*, 2003, 2004), which probably occurred due to the collision between the Indochina and South China Blocks (Chung *et al.*, 1999), and between the South China and North China Blocks (Li *et al.*, 1993). Since the early Jurassic, the Yangtze Block has been a stable continental platform, characterized by redbed sedimentation (Chen & Jahn, 1998). Mesozoic volcanic and intrusive rocks are widely exposed

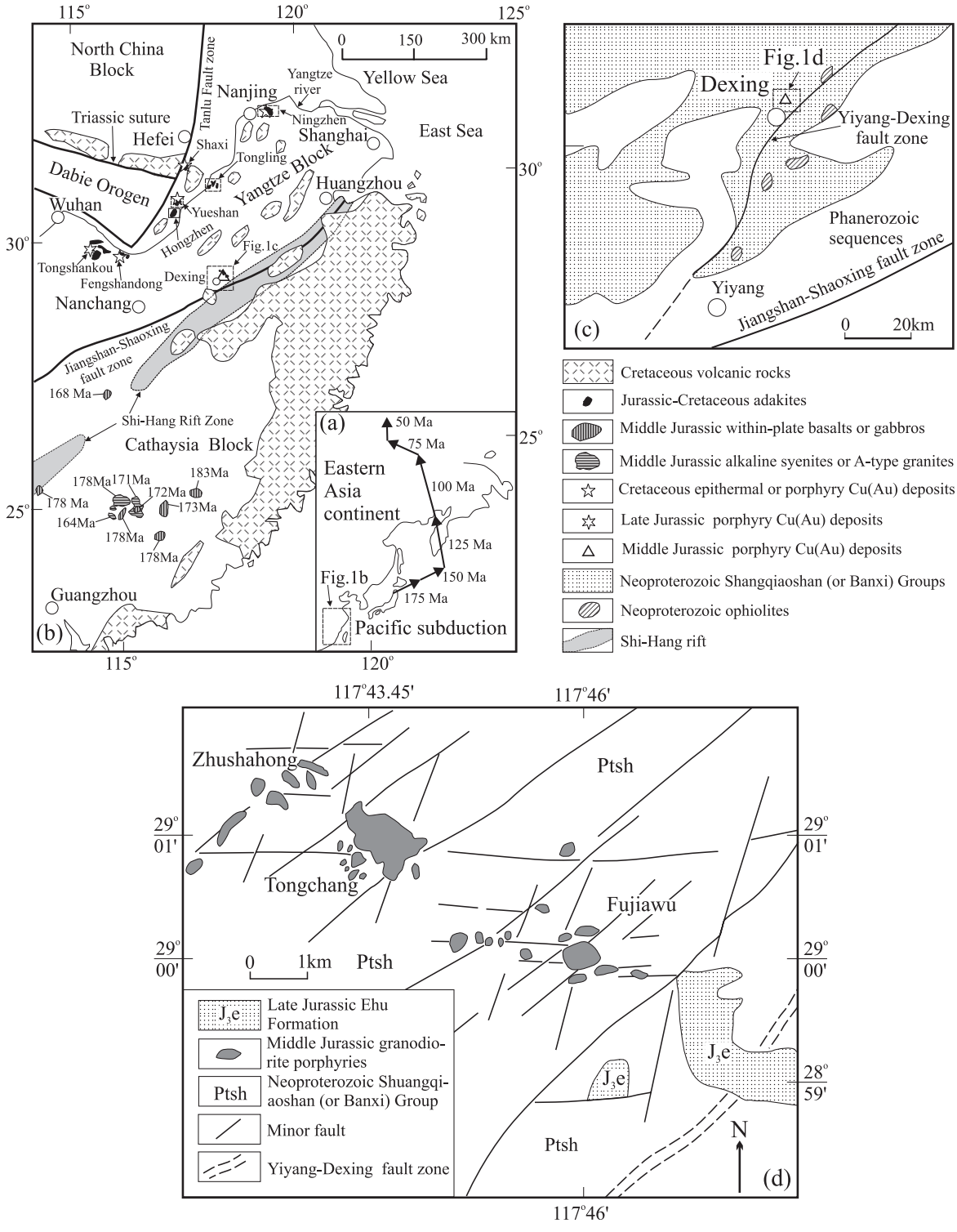

Fig. 1. Geological setting of the Dexing and adjacent areas. (a) The convergence vectors for late Mesozoic to early Cenozoic (175–50 Ma) subduction of the northwestern Pacific Plate beneath Asia (after Ratschbacher *et al.*, 2000). (b) Geological sketch map of South China: data for Jurassic–Cretaceous adakites in the eastern Yangtze Block are after Wang (2000), Zhang *et al.* (2001), Xu *et al.* (2002), Wang *et al.* (2003*a*, 2003*c*, 2004) and this study; data for Middle Jurassic within-plate basalts, gabbros, alkaline syenites or A-type granites in the Cathaysia Block are after Li *et al.* (2003, 2004) and Wang *et al.* (2003*b*, 2004*c*). (c) Geological sketch map of the Dexing and adjacent area, showing the distribution of Neoproterozoic ophiolites (after Li *et al.*, 1997). (d) Geological sketch map of the Dexing area, showing distribution of Middle Jurassic adakitic porphyries.

in the eastern Yangtze Block (e.g. Jurassic to Cretaceous diorite, quartz diorite, granodiorite, granite; Gilder *et al.*, 1996; Chen & Jahn, 1998; Xu *et al.*, 1999; Zhou & Li, 2000; Li *et al.*, 2003, 2004); these include the Dexing adakitic porphyries, which are the focus of this study.

The Dexing area lies in the eastern part of the Yangtze Block (Fig. 1b), to the north of the Jiangshan–Shaoxing fault zone, and is transected by the Yiyang–Dexing fault zone in its southeastern part (Fig. 1c). Ophiolitic melanges (~1000 Ma) are distributed along the Yiyang–Dexing fault zone (Fig. 1c), which represents a subordinate Neoproterozoic suture zone between the Yangtze continental block and an oceanic island arc (Chen *et al.*, 1991; Li *et al.*, 1997). To the east of Dexing (Fig. 1b), the NE-trending Jurassic–Cretaceous Shi–Hang rift zone parallels the Jiangshan–Shaoxing suture; this is marked by a series of NE-trending Jurassic–Cretaceous extensional basins, and abundant Middle–Late Jurassic (184–152 Ma) A-type granites, within-plate basalts and gabbros (Gilder *et al.*, 1996; Zhao *et al.*, 2001; Li *et al.*, 2003, 2004; Wang *et al.*, 2003*b*, 2004*c*).

The Dexing porphyry copper deposits occur 50 km NW of the Shi–Hang rift zone (Fig. 1b), and are hosted in three porphyries: the Tongchang (0·7 km^2) in the central part of the area, Fujiawu (0·2 km^2) to the southeast, and Zhushahong (0·06 km^2) in the northwest (Zhu *et al.*, 1983; He *et al.*, 1999). Copper reserves in the Dexing area are estimated at over 10 million metric tons, and the Tongchang porphyry deposit is the largest in China (Zhu *et al.*, 1983; Rui *et al.*, 1984; Goodell *et al.*, 1991).

Rhyolites and tuffs of the late Jurassic Ehu Formation have been recognized in the Dexing area (Fig. 1d), but, to date, no contemporary basaltic or gabbroic rocks have been found. The wall rocks of the porphyries and the related porphyry Cu deposits are epizonal metamorphic rocks (e.g. slate, tuffaceous phyllite and breccia) of the Neoproterozoic Shuangqiaoshan Group (Fig. 1d). The Dexing adakitic porphyries are characterized by extensive alteration similar to that associated with Cu–Au porphyry deposits worldwide (He *et al.*, 1999). In general, the most extensive alteration occurs in the contact zone between the porphyries and the wall rocks, and decreases on either side of the contact.

PETROGRAPHY

The granodiorite and quartz-diorite porphyries in the Dexing area are characterized by idiomorphic phenocrysts of andesine (An = 30–45), 0·5–4 mm in length, which exhibit weak normal zoning. Other phenocryst minerals are idiomorphic–hypidiomorphic hornblende (0·5–2 mm) and biotite (0·5–3 mm), tabular K-feldspar (1–5 mm) and quartz (1–3 mm). The matrix has a microgranular or fine granular (0·05–0·3 mm grain size) texture and consists of hypidiomorphic oligoclase (An = 16–20), hornblende and biotite, and xenomorphic quartz and K-feldspar. The principal and accessory mineral contents of the different intrusives in the Dexing area show only small variation. For example, the Tongchang intrusive rocks consist of plagioclase (46–52%), quartz (16–23%), K-feldspar (14–17%), amphibole (7–11%) and biotite (2–9%). The panning of placer minerals indicates that the accessory minerals in these rocks include magnetite (8763 g/t (gram/ton)), apatite (2546 g/t), titanite (1192 g/t), and rare ilmenite (196 g/t), zircon (124 g/t), pyrite (174 g/t), chalcopyrite (200 g/t) and molybdenite 2 g/t (Zhu *et al.*, 1983; Rui *et al.*, 1984). The Fujiawu intrusive rocks comprise plagioclase (43–55%), quartz (18–23%), K-feldspar (13–18%), amphibole (7–10%) and biotite (3–7%). Their accessory minerals include magnetite (5261 g/t), apatite (351 g/t), titanite (145 g/t), and zircon (194 g/t) (Zhu *et al.*, 1983; Rui *et al.*, 1984). The Zhushahong intrusive rocks are composed of plagioclase (47–52%), quartz (19–21%), K-feldspar (13–16%), amphibole (8–10%) and biotite (4–7%). Their accessory minerals include magnetite (434 g/t), apatite (673 g/t), and zircon (56 g/t) (Zhu *et al.*, 1983; Rui *et al.*, 1984). Magnetite is the dominant accessory mineral in the Dexing adakitic porphyries. In addition, anhydrite (1–2%) has also been recognized in some of the adakitic porphyries.

ANALYTICAL METHODS

Samples from the Tongchang, Fujiawu and Zhushahong porphyritic intrusives were initially examined by optical microscopy; unaltered or the least altered samples were selected for further analysis.

Zircons were separated using conventional heavy liquid and magnetic separation techniques. Representative zircon grains were handpicked and mounted in an epoxy resin disc, and then polished and coated with gold film. Their internal morphology was examined using cathodoluminescence prior to U–Pb isotopic analysis. The U–Pb isotopic analyses were performed using the Sensitive High-Resolution Ion Microprobe (SHRIMP-II) at the Chinese Academy of Geological Sciences, Beijing, following the procedures described by Jian *et al.* (2003). For the zircon analyses, nine ion species of Zr_2O^+, $^{204}Pb^+$, background, $^{206}Pb^+$, $^{207}Pb^+$, $^{208}Pb^+$, U^+, Th^+, ThO^+ and UO^+ were measured on a single electron multiplier by cyclic stepping of the magnetic field, recording the mean ion counts of every five scans. A primary ion beam of ~4·5 nA, 10 kV O^{2-} and ~25–30 μm spot diameter was used. Interelement fractionation in the ion emission of zircon was corrected for using the RSES reference standard TEM (417 Ma). The software of Ludwig (SQUID1.0) and accompanying ISOPLOT were used for data processing (Ludwig, 1999, 2001). Ages were calculated using the constants recommended

Table 1: SHRIMP U–Pb isotopic data for zircons from the Tongchang and Fujiawu adakitic granodiorite porphyries

Spot	$^{206}Pb_c$ (%)	U (ppm)	Th (ppm)	$^{232}Th/^{238}U$	$^{206}Pb^*$ (ppm)	$^{206}Pb/^{238}U$ (age, Ma)	$^{207}Pb^*/^{206}Pb^*$	±%	$^{207}Pb^*/^{235}U$	±%	$^{206}Pb^*/^{238}U$	±%
Tongchang												
F1·1	1·40	489	357	0·76	11·20	165·5 ± 4·5	0·0385	15	0·138	16	0·02601	2·8
F2·1	2·08	445	284	0·66	10·20	164·6 ± 4·5	0·0448	16	0·160	16	0·02586	2·8
F3·1	2·30	529	268	0·52	12·70	170·6 ± 4·6	0·0362	21	0·134	22	0·02682	2·8
F4·1	—	418	216	0·54	10·20	171·6 ± 4·8	0·0285	30	0·106	30	0·02697	2·8
F5·1	—	419	196	0·48	9·93	171·3 ± 4·7	0·0501	12	0·186	12	0·02693	2·8
F6·1	—	501	269	0·55	12·00	169·7 ± 5·1	0·0440	34	0·160	34	0·02667	3·0
F7·1	—	446	248	0·57	10·60	171·6 ± 4·7	0·0494	13	0·184	13	0·02697	2·8
F8·1	—	531	228	0·44	12·70	171·0 ± 4·6	0·0392	18	0·145	18	0·02688	2·7
F8·2	—	402	222	0·57	9·62	172·0 ± 4·8	0·0465	13	0·173	13	0·02704	2·8
F9·1	—	1097	1221	1·15	26·40	176·7 ± 4·4	0·0516	4·0	0·198	4·7	0·02778	2·6
F10·1	—	201	90	0·46	5·02	175·6 ± 5·4	0·0550	21	0·210	21	0·02761	3·1
F11·1	—	539	316	0·61	13·60	171·8 ± 5·2	0·0440	30	0·165	30	0·02701	3·1
F12·1	—	298	199	0·69	7·17	167·5 ± 6·2	0·0540	29	0·198	29	0·02632	3·7
F13·1	—	655	373	0·59	15·80	172·8 ± 4·6	0·0428	12	0·160	12	0·02717	2·7
F14·1	—	566	310	0·57	13·30	169·8 ± 4·5	0·0498	12	0·183	13	0·02670	2·7
Fujiawu												
B2·1	—	622	274	0·46	15·00	176·4 ± 4·6	0·0550	6·4	0·211	6·9	0·02775	2·7
B2·2	—	442	193	0·45	10·50	173·2 ± 4·7	0·0568	10	0·213	11	0·02723	2·7
B3·1	—	413	176	0·44	9·92	172·9 ± 4·7	0·0507	11	0·190	12	0·02719	2·8
B4·1	—	434	166	0·39	10·10	167·7 ± 4·6	0·0483	14	0·176	14	0·02636	2·8
B5·1	—	854	263	0·32	20·00	172·0 ± 4·7	0·0508	6·5	0·189	7·1	0·02705	2·8
B6·1	—	508	210	0·43	12·00	172·0 ± 4·5	0·0569	8·1	0·212	8·6	0·02703	2·7
B7·1	—	400	152	0·39	9·38	168·3 ± 4·7	0·0459	19	0·167	19	0·02645	2·9
B7·2	—	414	171	0·43	9·61	167·1 ± 4·6	0·0483	16	0·175	16	0·02625	2·8
B8·1	—	493	212	0·44	11·60	173·1 ± 4·6	0·0585	9·1	0·219	9·5	0·02721	2·7
B9·1	—	675	300	0·46	15·70	168·6 ± 4·5	0·0450	14	0·165	14	0·02650	2·7
B10·1	—	367	157	0·44	8·53	169·2 ± 4·5	0·0649	8·0	0·238	8·5	0·02660	2·7
B11·1	—	565	252	0·46	13·20	168·6 ± 4·5	0·0484	11	0·177	11	0·02650	2·7
B12·1	—	584	264	0·47	13·40	165·5 ± 4·7	0·0453	12	0·162	12	0·02601	2·9
B13·1	—	443	188	0·44	10·40	169·6 ± 4·7	0·0516	14	0·189	14	0·02665	2·8
B14·1	—	436	175	0·41	10·50	172·4 ± 4·7	0·0442	16	0·165	16	0·02711	2·8

(1) Errors are 1σ; Pb_c and Pb* indicate the common and radiogenic portions, respectively. (2) Error in standard calibration was 0·33% (not included in above errors but required when comparing data from different mounts). (3) Common Pb corrected using measured ^{204}Pb.

by IUGS (Steiger & Jager, 1977). Uncertainties in the ages listed in Table 1 are cited as 1σ, and the weighted mean ages are quoted at the 95% confidence level.

The samples chosen for elemental and isotopic analysis were first split into small chips and soaked in 4N hydrochloric acid for one hour to remove secondary carbonate minerals, then were powdered after rinsing with distilled water. Major elements were analyzed at the Hubei Institute of Geology and Mineral Resources by wavelength dispersive X-ray fluorescence spectrometry. Analytical errors are less than 2%. FeO contents of the samples were determined by conventional wet chemical titration methods. The analytical procedures used to determine FeO and the other major elements have been described in detail by Gao *et al.* (1995). Trace elements, including the rare earth element (REE), were analyzed using a Perkin-Elmer ELAN 6000 inductively coupled plasma source mass spectrometer (ICP-MS) at the Guangzhou Institute of Geochemistry, Chinese Academy of Sciences, following procedures described by Li *et al.* (2002*b*). Analytical precision for most elements is better than 3%.

Sr and Nd isotopic compositions were determined using a Finnigan MAT-262 mass spectrometer operated in a static multi-collector mode at the Institute of Geology

and Geophysics, Chinese Academy of Sciences, Beijing, following procedures similar to those of Zhang *et al.* (2002). The $^{87}Sr/^{86}Sr$ ratio of NBS standard 987 and the $^{143}Nd/^{144}Nd$ ratio of the La Jolla standard measured during the period of analysis were 0·710234 ± 7 ($2\sigma_m$) and $^{143}Nd/^{144}Nd$ = 0·511838 ± 8 ($2s_m$), respectively. Procedural blanks were about 50 pg for Sm and Nd and 0·2–0·5 ng for Rb and Sr. The Rb, Sr, Sm and Nd concentrations were also measured by isotope dilution; the concentrations exhibit good agreement with the data obtained by ICP-MS. The measured $^{143}Nd/^{144}Nd$ and $^{86}Sr/^{88}Sr$ ratios were normalized to $^{143}Nd/^{144}Nd$ = 0·7219 and $^{86}Sr/^{88}Sr$ = 0·1194, respectively.

RESULTS

SHRIMP U–Pb zircon geochronology

The analyzed zircons from two Dexing adakitic porphyry samples (01TC-1 and 01FJW-1–2) are mostly prismatic (about 200–350 mm length) with well-developed pyramidal faces. Cathodoluminescence images clearly show micro-scale oscillatory zoning (Fig. 2), which implies a magmatic origin for the zircons. No overgrowth rim is observed. The results of SHRIMP U–Pb zircon analyses for the Tongchang (sample 01TC-1) and Fujiawu (sample 01FJW-1–2) granodiorite porphyries are listed in Table 1 and illustrated on a concordia plot in Fig. 2. Zircons from sample 01TC-1 have variable U (201–1097 ppm) and Th (90–1221 ppm) contents, but possess typical igneous Th/U ratios (0·43–1·11) (Table 1), whereas zircons from sample 01FJW-1–2 have relatively uniform concentrations of U (400–675 ppm) and Th (152–300 ppm), and also show typical igneous Th/U ratios (0·31–0·45) (Table 1). For zircons from sample 01TC-1, all 15 analyses, including points in both the core and rim of the zircons, have U–Pb isotopic compositions that are concordant and indistinguishable from each other, resulting in a single age population with a weighted mean $^{206}Pb/^{238}U$ age of 171 ± 3 Ma (2σ) (MSWD = 0·47) (Table 1; Fig. 2). Similarly, for zircons from sample 01FJW-1–2, all 15 analyses, including points in both the core and rim of the zircons, also yield a single age population with a weighted mean $^{206}Pb/^{238}U$ age of 171 ± 3 Ma (2σ) (MSWD = 0·40) (Table 1; Fig. 2). The identical ages (within error) of both the Tongchang and Fujiawu granodiorite porphyries indicate that they could have formed in the same magmatic event. Drilling data suggest that the Zhushahong intrusive body is linked to the Tongchang intrusive at about 1000 m depth (Zhu *et al.*, 1983); consequently, the age of the Zhushahong granodiorite porphyry is deduced to be the same as that of the Tongchang granodiorite porphyry (about 171 ± 3 Ma). In addition, Re–Os isotope dating of molybdenite from the Dexing porphyry Cu deposits also gives ~173 Ma (Mao & Wang, 2000), which is consistent with the formation age of the Dexing granodiorite porphyries, indicating that the Cu mineralization and the crystallization of the granodiorite porphyries in the Dexing area were approximately contemporaneous.

Alteration effects

The major and trace element compositions of the studied samples are listed in Table 2. Samples of the Dexing porphyries have variable LOI (loss on ignition) reflecting variable $H_2O + CO_2$ contents (1·12–5·44%) (Table 2; Zhu *et al.*, 1983; Rui *et al.*, 1984; Hua & Dong, 1984), possibly due to different degrees of alteration (e.g. Zhou, 1999). In general, the high-field-strength elements (HFSE), rare earth elements (REE), Th and transition elements are essentially immobile during the most intense hydrothermal alteration (e.g. Zhou, 1999; Hawkesworth *et al.*, 1997). Mg is thought to be easily transported in solution and its content will be changed by alteration in some mafic rocks containing olivine and pyroxene, but it tends to be immobile and will not be greatly affected by alteration in intermediate–acid igneous rocks due to the lack of olivine and pyroxene (e.g. Zhou, 1999). In addition, some major elements such as Ti, P, Al, Fe and Mn are not readily transported by hydrothermal alteration (e.g. Zhou, 1999), but Ca, Na, K and the large ion lithophile elements (e.g. Sr, Ba and Rb) are generally mobile (Smith & Smith, 1976). The Al_2O_3, FeO^T ($= Fe_2O_3 \times 0{\cdot}9 + FeO$), MgO, TiO_2, P_2O_5 and Th contents of the Dexing adakitic porphyries show no obvious variation with increasing LOI ($H_2O + CO_2$ contents) (Fig. 3a–f), indicating that their contents have probably not been changed by alteration; however, Na_2O and K_2O contents clearly decrease with increasing LOI (Fig. 3 g–h), implying the their original contents were modified by alteration. Thus, only immobile elements such as the high-field-strength elements (Ti, Zr, Y, Nb, Ta, Hf) and Th, Al_2O_3, FeO^T, MgO, P_2O_5, REE and transition elements are used in the following discussion.

The $^{143}Nd/^{144}Nd$ ratios of igneous rocks are seldom modified by hydrothermal alteration, but $^{87}Sr/^{86}Sr$ ratios can be markedly changed (e.g. Menzies *et al.*, 1993). In LOI vs $\varepsilon_{Nd(t)}$ and $(^{87}Sr/^{86}Sr)_i$ diagrams (Fig. 3i and j; Table 3), the $\varepsilon_{Nd(t)}$ values of the Dexing adakitic porphyries exhibit little variation with increasing LOI. On the other hand, variations in $(^{87}Sr/^{86}Sr)_i$ are complex; when LOI contents are less than 2·5%, $(^{87}Sr/^{86}Sr)_i$ ratios are relatively constant. However, when LOI increases to 5·44% (sample 01T-15), $(^{87}Sr/^{86}Sr)_i$ increases significantly. This implies that alteration (e.g. LOI > 2·5%) can cause the $(^{87}Sr/^{86}Sr)_i$ ratio of a rock to vary markedly (Jin *et al.*, 2002), whereas $\varepsilon_{Nd(t)}$ values remain stable. Therefore, we believe that the $(^{87}Sr/^{86}Sr)_i$ ratios of the Dexing adakitic porphyries with low LOI (<2·5%), and all $\varepsilon_{Nd(t)}$

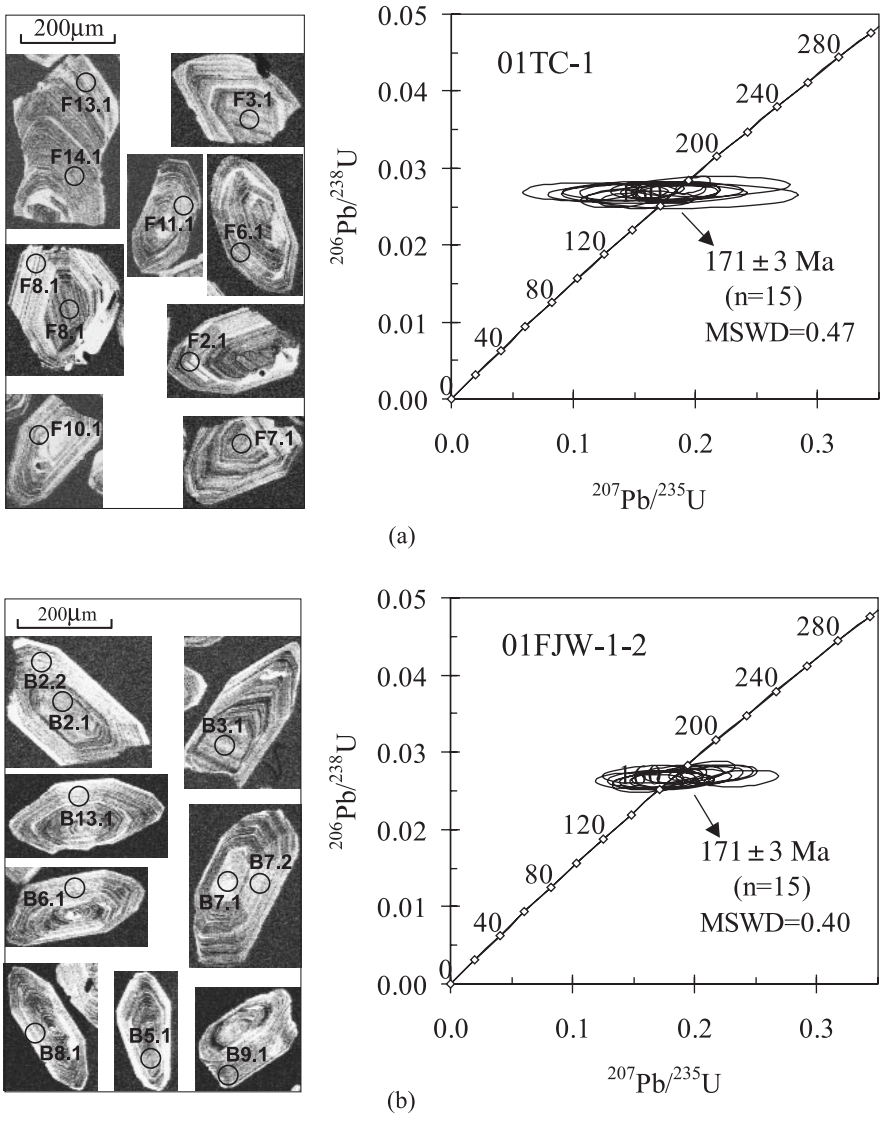

Fig. 2. SHRIMP zircon U–Pb concordia diagrams with cathodoluminescence electron images for samples 01TC-1 (Tongchang) (a) and 01FJW-1–2 (Fujiawu) (b).

values, probably represent the original isotopic signatures, except for sample 01T-15 with a high LOI value (>5·44%).

Major and trace element geochemistry

The major and trace element compositional characteristics and classification of the Dexing adakitic porphyries are shown in Figs 4 and 5. Fields of adakitic rocks inferred to be generated by slab melting and lower crustal melting are also plotted in Figs 4 and 5 for comparison. These have been classified into four sub-groups according to the different petrogenesis: (1) subducted oceanic crust-derived adakites that have interacted with mantle peridotite (Defant & Drummond, 1990; Kay *et al.*, 1993; Drummond *et al.*, 1996; Stern & Kilian, 1996; Sajona *et al.*, 2000; Aguillón-Robles *et al.*, 2001; Bourdon *et al.*, 2002; Martin *et al.*, 2005); (2) delaminated lower crust-derived adakitic rocks that have interacted with mantle peridotite (Kay & Kay, 1993; Defant *et al.*, 2002; Xu *et al.*, 2002; Wang *et al.*, 2004*a*, 2004*b*); (3) adakitic rocks directly derived from a thick crust (Atherton & Petford, 1993; Muir *et al.*, 1995; Petford & Atherton, 1996; Johnson *et al.*, 1997; Xiong *et al.*, 2003; Wang *et al.*, 2004*a*); (4) pure slab melts that have not interacted with mantle peridotite (Kepezhinskas *et al.*, 1995; Sorensen & Grossman, 1989). The Dexing porphyries are similar to these adakitic rocks and share the following compositional characteristics: (1) they exhibit a calc-alkaline compositional trend (Fig. 4a); (2) they show similar

Table 2: Major (wt %) and trace element (ppm) compositions of the adakitic porphyries in the Dexing area

No.:	1	2	3	4	5	6	7	8
Sample:	CK307-1	CK307-4	CK309-9	01FJW-1-1	01FJW-1-2	01FJW-2	01FJW-3	01FJW-4
SiO_2	64·63	65·83	65·75	68·25	67·82	61·29	68·08	67·33
TiO_2	0·43	0·42	0·38	0·43	0·46	0·63	0·44	0·41
Al_2O_3	15·48	15·22	15·14	15·22	15·38	15·25	15·33	15·19
Fe_2O_3	1·36	1·51	2·19	1·69	1·54	2·29	1·44	1·59
FeO	2·48	2·20	2·45	2·07	2·37	3·80	2·18	2·35
MnO	0·09	0·09	0·06	0·03	0·04	0·21	0·03	0·02
MgO	2·05	1·85	1·87	1·84	1·87	3·86	1·82	1·80
CaO	3·84	3·94	3·29	1·59	1·67	2·78	1·42	1·96
Na_2O	4·09	3·87	3·64	3·63	3·66	2·85	3·46	3·70
K_2O	3·11	3·04	3·13	3·02	2·93	1·79	3·38	3·47
P_2O_5	0·20	0·20	0·19	0·08	0·09	0·19	0·10	0·09
H_2O	1·37	1·04	1·34	1·82	1·79	3·59	1·95	1·60
CO_2	0·48	0·45	0·06	0·05	0·05	1·18	0·05	0·14
$\sum$	99·61	99·67	99·49	99·72	99·67	99·71	99·68	99·65
Mg-no.	50	48	43	48	47	54	48	46
Sc	8·42	9·79	8·99	7·81	7·90	15·8	7·38	7·64
V	74·2	75·2	74·3	67·5	66·2	135	62·4	69·4
Cr	54·0	42·2	37·1	33·3	41·8	80·1	35·1	30·2
Co	8·60	10·5	9·66	6·93	7·66	12·3	7·10	6·93
Ni	22·4	20·2	16·7	15·2	14·5	30·7	15·3	12·1
Ga	18·3	19·7	19·8	18·3	18·5	16·5	18·9	18·2
Rb	81·6	81·3	57·3	55·1	56·1	71·3	59·7	53·9
Sr	790	873	632	623	691	442	573	638
Y	11·3	10·2	8·34	6·77	8·35	13·0	6·01	5·84
Zr	112	100	85·4	172	164	108	144	122
Nb	9·76	9·92	7·71	7·85	7·78	8·32	8·73	7·20
Cs	3·70	4·96	2·86	3·96	4·13	23·62	3·82	3·93
Ba	1321	1288	1339	1203	1224	1273	1262	1257
Hf	3·08	3·13	2·74	4·49	4·31	2·97	3·95	3·20
Ta	0·76	0·83	0·66	0·71	0·69	0·72	0·72	0·65
Pb	11·4	9·76	10·3	13·4	12·1	16·3	12·6	10·3
Th	15·3	17·9	16·2	13·7	15·6	14·7	16·8	14·3
U	4·02	4·68	3·52	2·05	1·92	3·38	2·39	1·58
La	37·30	39·58	20·70	26·62	31·40	28·46	23·34	14·97
Ce	60·75	64·25	35·40	44·22	50·40	46·78	36·76	24·10
Pr	6·50	5·90	3·62	5·00	5·60	5·41	3·92	2·73
Nd	22·33	20·33	12·68	16·45	18·20	18·61	13·39	9·14
Sm	3·45	3·38	2·33	2·54	2·86	3·27	2·02	1·54
Eu	0·90	0·94	0·80	0·69	0·77	0·88	0·59	0·52
Gd	2·53	2·74	2·02	1·80	2·09	2·78	1·40	1·22
Tb	0·38	0·35	0·26	0·25	0·31	0·41	0·21	0·18
Dy	1·99	1·88	1·45	1·21	1·49	2·21	1·07	0·97
Ho	0·37	0·33	0·28	0·23	0·28	0·43	0·19	0·17
Er	1·00	0·92	0·86	0·61	0·75	1·14	0·54	0·49
Tm	0·15	0·14	0·12	0·10	0·11	0·18	0·08	0·08
Yb	1·01	0·98	0·75	0·68	0·82	1·17	0·59	0·55
Lu	0·17	0·15	0·11	0·12	0·14	0·20	0·10	0·09
Eu/Eu*	0·93	0·94	1·13	0·98	0·96	0·89	1·07	1·16
Sr/Y	70	86	76	92	83	34	95	109
La/Yb	37	40	28	39	38	24	39	27

No.:	9	10	11	12	13	14	15	16
Sample:	01FJW-5	01TC-01	01TC-02	01TC-03	01T-15	01T-16	01T-17	G-83-175
SiO_2	68·24	65·31	63·86	65·28	59·44	66·14	64·53	64·67
TiO_2	0·42	0·53	0·60	0·53	0·39	0·38	0·38	0·49
Al_2O_3	14·96	15·16	14·88	15·18	14·56	14·57	14·70	14·97
Fe_2O_3	1·59	0·96	2·45	0·99	1·34	1·33	2·16	1·55
FeO	2·05	3·25	3·75	3·02	2·80	2·30	2·73	2·60
MnO	0·03	0·04	0·06	0·12	0·08	0·07	0·06	0·11
MgO	1·67	2·93	3·23	2·43	2·40	1·95	2·23	2·35
CaO	1·74	2·03	1·83	2·24	5·85	3·70	2·88	4·50
Na_2O	4·03	2·24	1·69	3·51	4·26	3·77	4·28	3·57
K_2O	2·87	2·40	2·36	2·10	2·84	3·20	3·13	3·30
P_2O_5	0·06	0·18	0·19	0·08	0·23	0·19	0·22	0·26
H_2O	1·69	3·20	3·70	2·25	2·45	1·20	1·66	1·23
CO_2	0·24	1·06	1·06	1·53	2·91	0·50	0·56	0·07
$\sum$	99·59	99·29	99·66	99·26	99·55	99·30	99·51	99·67
Mg-no.	46	56	49	53	52	50	46	51
Sc	7·12	11·1	11·7	8·28	9·76	9·39	8·23	9·28
V	69·0	95·4	101	76·3	79·0	75·9	75·4	74·1
Cr	37·9	72·9	73·4	59·7	50·8	43·3	46·3	56·2
Co	7·86	19·9	8·67	10·4	9·93	9·65	9·22	10·4
Ni	13·4	32·8	28·7	21·0	22·3	18·3	22·7	23·8
Ga	18·2	17·3	19·0	16·8	17·2	17·8	18·6	17·6
Rb	52·3	114	136	89·1	109	114	119	104
Sr	713	1318	648	1833	916	651	656	818
Y	2·81	10·0	9·05	7·68	11·0	9·59	8·63	13·43
Zr	113	127	160	97·1	111	77·4	83·3	41·4
Nb	6·36	9·13	10·0	8·56	8·98	10·5	9·34	10·4
Cs	7·14	30·4	27·2	17·0	32·5	5·60	4·81	1·72
Ba	1420	1550	1431	3959	933	1124	1205	1465
Hf	3·06	3·43	4·28	2·79	3·26	2·57	2·49	1·59
Ta	0·65	0·78	0·85	0·74	0·84	0·76	0·80	0·86
Pb	8·92	31·0	11·2	9·05	6·85	9·06	8·11	8·27
Th	12·6	18·2	18·0	17·7	18·0	27·2	19·8	20·5
U	1·50	4·84	3·02	4·11	3·39	5·43	3·00	5·08
La	9·31	33·62	29·60	31·46	45·76	58·37	28·70	41·26
Ce	13·42	54·30	48·42	48·64	71·73	86·31	44·77	72·10
Pr	1·42	6·01	5·36	5·20	6·47	7·38	4·72	8·25
Nd	4·63	19·63	17·39	16·29	21·40	24·22	16·25	27·12
Sm	0·71	2·94	2·60	2·54	3·43	3·42	2·45	4·32
Eu	0·42	0·80	0·64	0·54	1·07	0·98	0·70	1·09
Gd	0·61	2·19	1·92	1·94	2·87	2·67	1·87	3·10
Tb	0·08	0·33	0·28	0·27	0·37	0·34	0·27	0·48
Dy	0·42	1·76	1·48	1·38	2·06	1·75	1·46	2·37
Ho	0·08	0·33	0·29	0·26	0·38	0·28	0·27	0·45
Er	0·23	0·92	0·78	0·70	1·18	0·93	0·75	1·18
Tm	0·04	0·15	0·13	0·12	0·16	0·14	0·11	0·17
Yb	0·28	1·02	0·93	0·80	1·02	0·89	0·73	1·19
Lu	0·05	0·18	0·17	0·14	0·18	0·15	0·12	0·19
Eu/Eu*	1·93	0·96	0·88	0·75	1·05	0·99	1·00	0·91
Sr/Y	254	132	72	239	83	68	76	61
La/Yb	33	33	32	39	45	65	39	35

Nos 1–9: Fujiawu pluton; nos 10–15: Tongchang pluton; no. 16: Zhushahong. Samples 01FJW-3, 01TC-3 and G-83-175 from Wang *et al.* (2003*a*); all other samples are from this study.

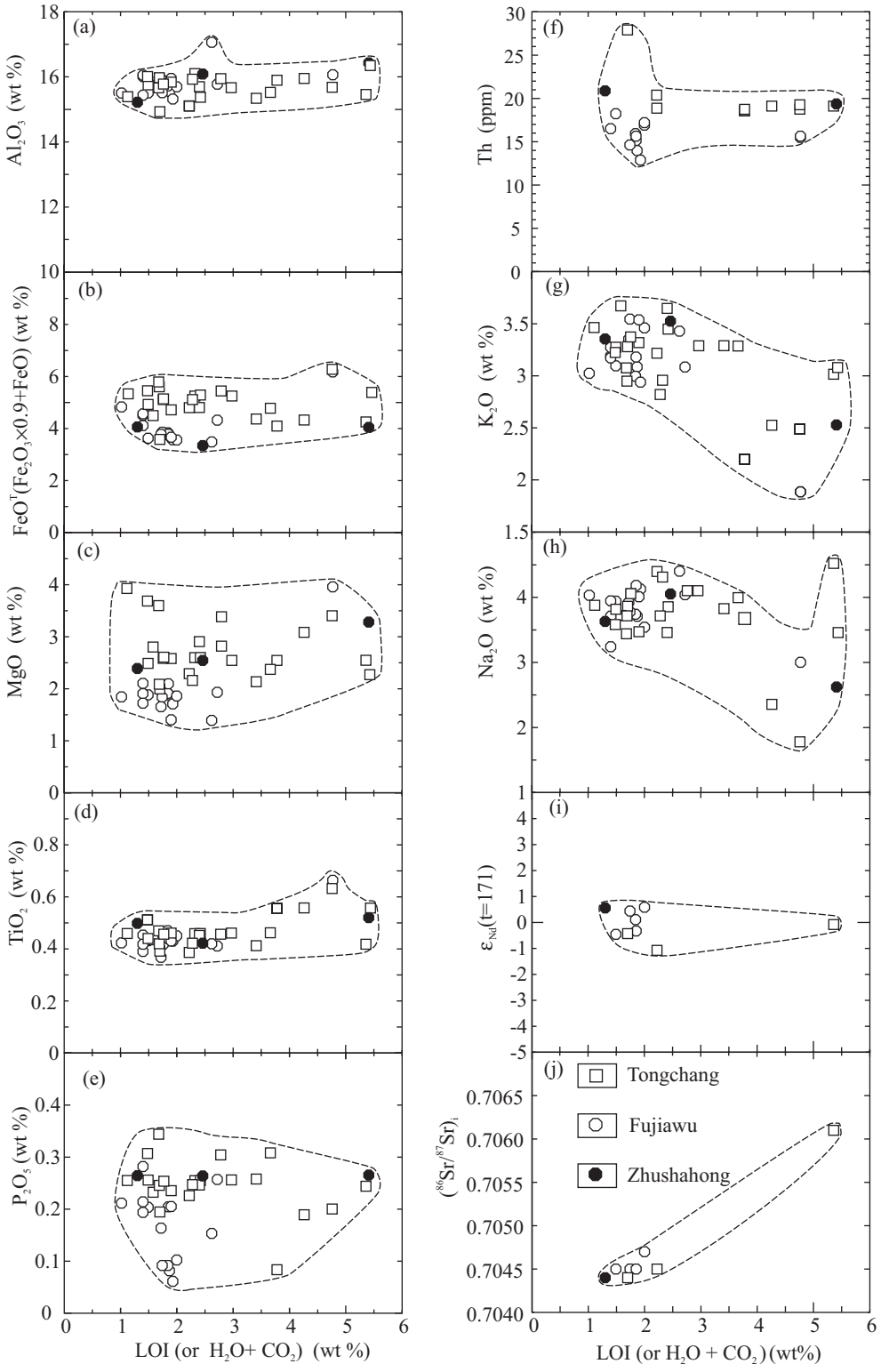

Fig. 3. LOI (loss on ignition) or CO_2 + H_2O versus major elements and Nd and Sr isotopic composition. The data for the Dexing adakitic porphyries are from Zhu *et al.* (1983), Rui *et al.* (1984), Hua *et al.* (1984) and Table 2.

Table 3: Nd–Sr isotopic compositions of the Dexing adakitic porphyries

Sample:	01FJW-1-2	01FJW-3	01FJW-4	CK307-1	CK307-4	G-83-175	01T-15	01T-16	01T-17	D01
Sm (ppm)	2·862	2·034	1·540	3·883	3·524	4·316	3·673	3·260	2·667	
Nd (ppm)	18·20	12·77	9·14	25·56	23·06	27·12	24·35	24·58	16·69	
$^{147}Sm/^{144}Nd$	0·0956	0·0969	0·1025	0·0919	0·0924	0·0968	0·0912	0·0797	0·0967	0·0972
$^{143}Nd/^{144}Nd$	0·512530	0·512557	0·512555	0·512504	0·512498	0·512555	0·512516	0·512485	0·512468	0·512619
$2\sigma_m$	±11	±11	±12	±4	±4	±09	±04	±12	±09	±09
$\varepsilon_{Nd}(t)$	0·11	0·59	0·44	−0·33	−0·46	0·56	−0·08	−0·43	−1·14	1·80
T_{DM}(Ga)	0·80	0·77	0·82	0·81	0·82	0·78	0·79	0·76	0·89	0·70
Rb (ppm)	56·12	61·60	53·92	84·78	80·29	103·7	110·2	114·1	122·8	
Sr (ppm)	690·8	573·8	638·4	801·2	792·5	817·6	931·0	724·6	582·6	
$^{87}Rb/^{86}Sr$	0·2350	0·3105	0·2443	0·3062	0·2932	0·3669	0·3426	0·4558	0·6098	
$^{87}Sr/^{86}Sr$	0·705028	0·705409	0·705110	0·705245	0·705195	0·705297	0·706942	0·705511	0·705958	
$2\sigma_m$	±18	±18	±14	±11	±8	±16	±4	±11	±11	
$(^{87}Sr/^{86}Sr)_i$	0·7045	0·7047	0·7045	0·7045	0·7045	0·7044	0·7061	0·7044	0·7045	

Sample D0I is from Zhu *et al*. (1990); other data are from this study.

geochemical characteristics (e.g. relatively low Yb contents and high La/Yb ratios) to Archean tonalite–trondhjemite–granodiorites (TTG) in Fig. 4b; (3) they have similar TiO_2 and P_2O_5 contents (Fig. 5a and b).

The Dexing adakitic porphyries exhibit relatively low FeO^T/MgO (1·16–2·68) ratios and Al_2O_3 (14·50–17·50%) contents (Fig. 5c and d), and relatively high MgO (1·80–5·00%), Cr (30–120 ppm), Ni (12–36 ppm) and Yb (0·28–1·40 ppm) contents (Fig. 5e–h; Table 2), compared with either thick lower crust-derived adakitic rocks or pure slab melts, similar to those of subducted oceanic crust-derived adakites and delaminated lower crust-derived adakitic rocks. In SiO_2 vs Th and Th/Ce diagrams (Fig. 5i and j), the Dexing adakitic porphyries clearly exhibit higher Th (12·6–27·2 ppm) contents and Th/Ce (0·19–0·94) ratios than those of subducted oceanic crust-derived adakites; however, some of the Dexing adakitic samples overlap with the field of the delaminated lower crust-derived adakitic rocks.

Chondrite-normalized REE patterns show that all samples of the Dexing adakitic porphyries are enriched in light REE (LREE) and depleted in heavy REE (HREE) (Fig. 6a and b), except for sample 01FJW-5, which clearly shows a positive Eu anomaly and concavity in the middle rare earth element (MREE) pattern; other samples have no obvious Eu anomalies, and only weakly concave MREE patterns (Fig. 6a and b). It is commonly considered that MREE patterns with clear to weak concavities imply the presence of residual amphibole in the source (Gromet & Silver, 1987). In addition, N-MORB normalized trace element patterns show that all samples are depleted in Nb and Ta and enriched in Sr (Fig. 6c and d). Although hydrothermal alteration may result in loss of Sr (e.g. Zhou, 1999), the Sr concentration of the Dexing adakitic porphyries is still rather high (442–2301 ppm) (Table 2), and this probably represents minimum values if the original concentrations have, in fact, reduced by hydrothermal alteration. The Dexing adakitic porphyries, therefore, clearly possess high Sr/Y ratios (34–254) and positive Sr anomalies, similar to adakites. Moreover, except for Th, the REE and trace element patterns of the Dexing adakitic porphyries are similar to those of subducted oceanic crust-derived adakites and delaminated lower crust-derived adakitic rocks, but unlike those of adakitic rocks directly derived from partial melting of a thickened crust or pure slab melts (Fig. 6).

Nd and Sr isotopes

The Dexing adakitic porphyries have relatively homogeneous $\varepsilon_{Nd}(t)$ values ranging from −1·14 to +1·80 and Nd model age (T_{DM}) ranging from 0·70 to 0·89 Ga (Table 3). Except for sample 01T-15, which has a high initial $^{87}Sr/^{86}Sr$ ratio (0·7061) due to alteration, all the other samples have relatively homogeneous initial $^{87}Sr/^{86}Sr$ (at $T = 171$ Ma) ratios ranging from 0·7044 to 0·7047 (Table 3). Compared with other late Mesozoic (180–90 Ma) mafic to acid igneous rocks, including Late Jurassic–Cretaceous adakitic rocks, in the eastern Yangtze Block (Chen & Jahn, 1998; Wang, 2000; Xu *et al*., 2002; Wang *et al*., 2003*a*, 2003*c*, 2004*a*, 2004*b*), the Dexing adakitic porphyries have the highest $\varepsilon_{Nd}(t)$ and the lowest initial $^{87}Sr/^{86}Sr$ ratios (Fig. 7a). Nevertheless, they have much lower $\varepsilon_{Nd}(t)$ than those of 400–179 Ma MORB (Mahoney *et al*., 1998; Xu *et al*., 2003; Tribuzio *et al*., 2004; Xu & Castillo, 2004) and Cenozoic adakites formed by slab melting (Defant *et al*., 1992; Kay *et al*., 1993; Sajona *et al*., 2000; Aguillón-Robles *et al*.,

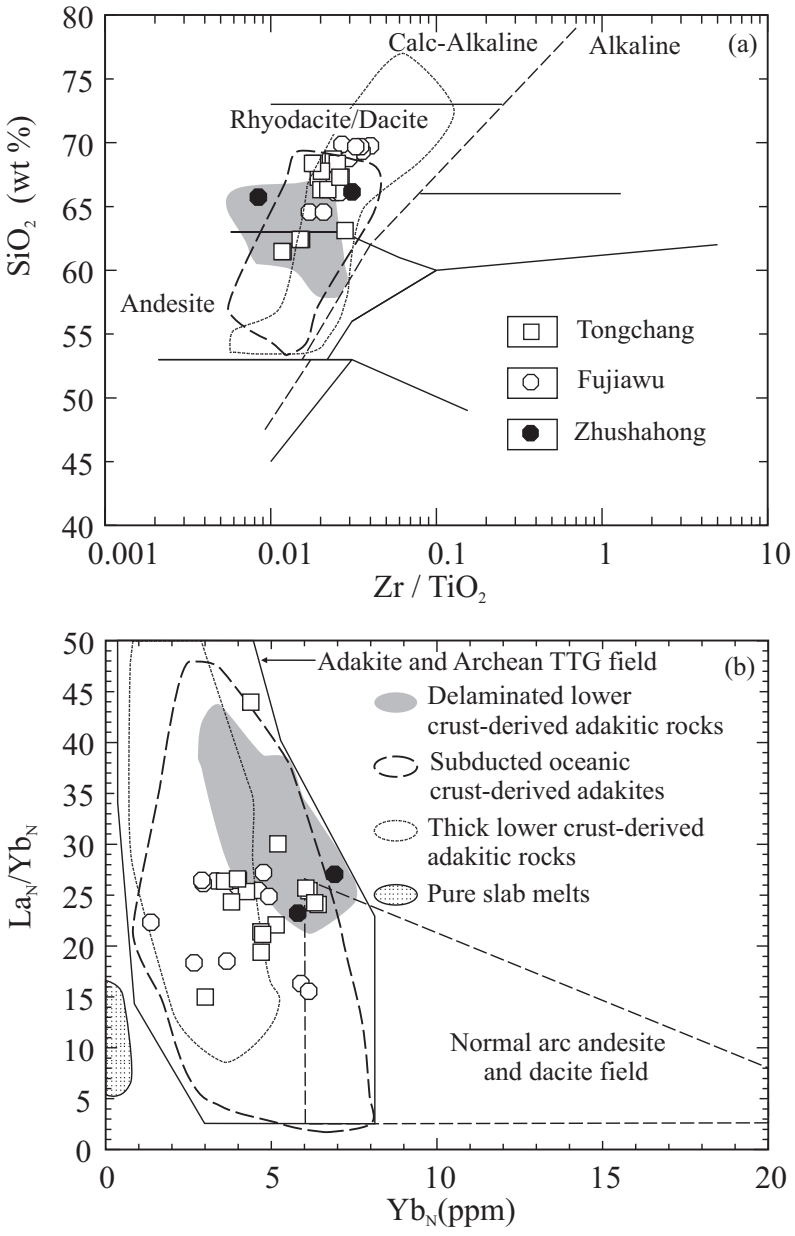

Fig. 4. (a) Chemical composition of the Dexing adakitic porphyries plotted in the Zr/TiO_2 vs SiO_2 classification diagram of Winchester & Floyd (1977). The dashed line separates calc-alkaline and alkaline compositions. (b) La_N/Yb_N vs Yb_N diagram (after Drummond & Defant (1990)). Data for the Dexing adakitic porphyries are after Zhu *et al.* (1983), Rui *et al.* (1984), Hua *et al.* (1984) and Table 2. Data for delaminated lower crust-derived adakitic rocks are from Xu *et al.* (2002) and Wang *et al.* (2004*a*, 2004*b*). The field of subducted oceanic crust-derived adakites is constructed using data from the following: Defant & Drummond (1990); Kay *et al.* (1993); Drummond *et al.* (1996); Stern & Kilian (1996); Sajona *et al.* (2000); Aguillón-Robles *et al.* (2001); Defant *et al.* (2002); Martin *et al.* (2005), and references therein. Data for thick lower crust-derived adakitic rocks are from the following: Atherton & Petford (1993); Muir *et al.* (1995); Petford & Atherton (1996); Johnson *et al.* (1997); Xiong *et al.* (2003). Pure slab melts are after Kepezhinskas *et al.* (1995) and Sorensen & Grossman (1989).

2001) (Fig. 7). On the other hand, samples of the Dexing adakitic porphyries plot in the field of Middle Jurassic (168–178 Ma) within-plate basalts and gabbros in the Cathaysia Block (Li *et al.*, 2003, 2004; Wang *et al.*, 2003*b*, 2004*c*), and adakitic rocks derived from partial melting of newly underplated basaltic lower crust (e.g. Separation Point Batholith of New Zealand (Muir *et al.*, 1995) and Cordillera Blanca Batholith of Peru (Atherton & Petford, 1993; Petford & Atherton, 1996)) (Fig. 7). They also fall in the field of Proterozoic ophiolites to the east of the Dexing area in Fig. 7b. In addition, although some samples of the Dexing adakitic porphyries

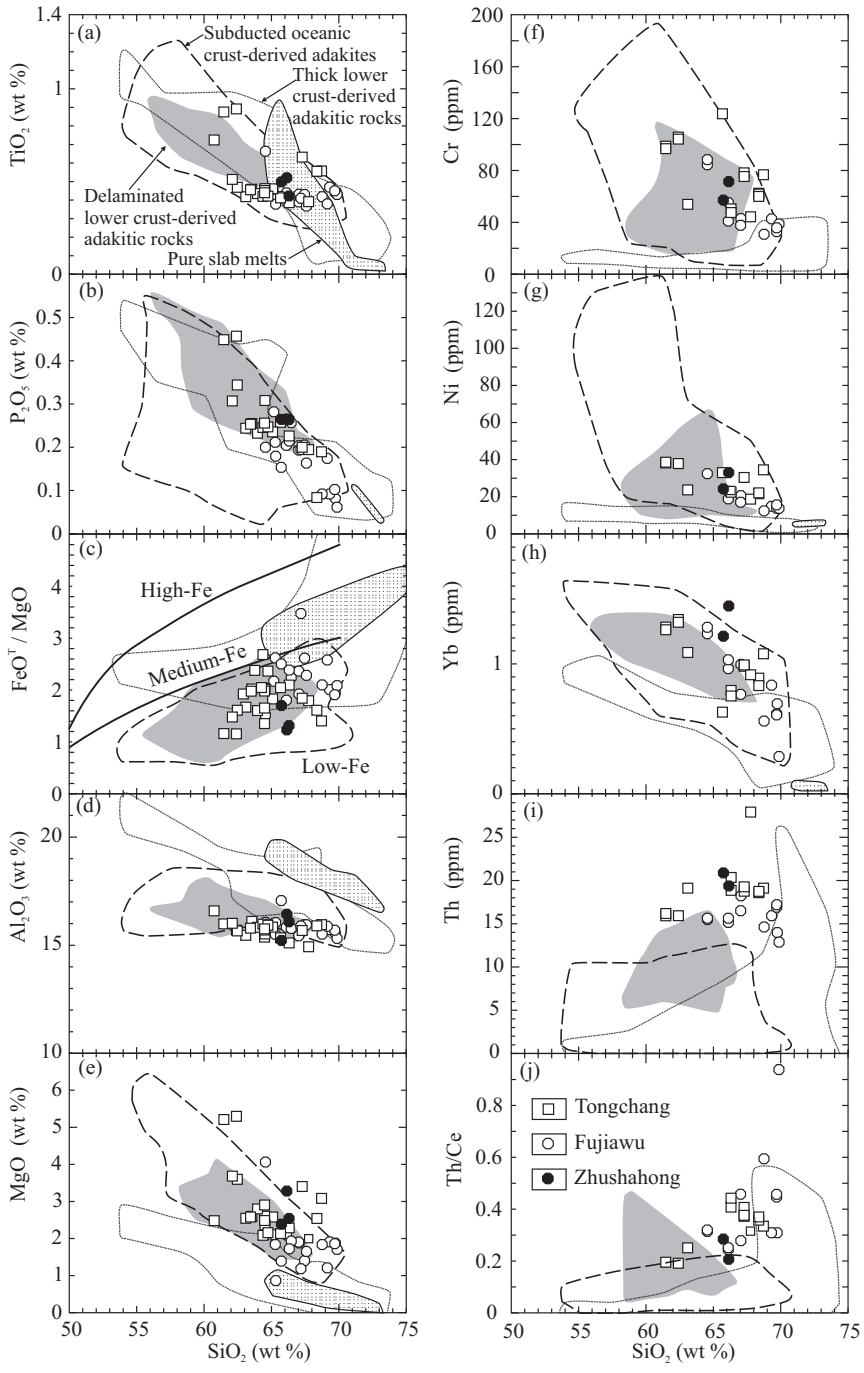

Fig. 5. Harker variation diagrams showing the major and trace element variations of the Dexing adakitic porphyries. The discriminant boundaries (bold lines) between low-, medium- and high-Fe igneous rocks suites in (c) are from Arculus (2003). Data for the Dexing adakitic porphyries are after Zhu *et al.* (1983), Rui *et al.* (1984), Hua *et al.* (1984) and Table 2. The fields of delaminated lower crust-derived adakitic rocks, subducted oceanic crust-derived adakites, thick lower crust-derived adakitic rocks, and pure slab melts are constructed using the same data sources as in Fig. 4.

have $\varepsilon_{Nd}(t)$ close to those of some Proterozoic metamorphic rocks from the Yangtze Block (Figs 7b and 8), all samples have clearly lower T_{DM} than those of the Proterozoic metamorphic rocks and the Paleozoic sedimentary cover rocks from the Yangtze Block (e.g. Chen & Jahn, 1998; Fig. 7b). Moreover, the Dexing porphyries have clearly higher $\varepsilon_{Nd}(t)$ than those of all the Paleozoic–Mesozoic granitoids in the eastern

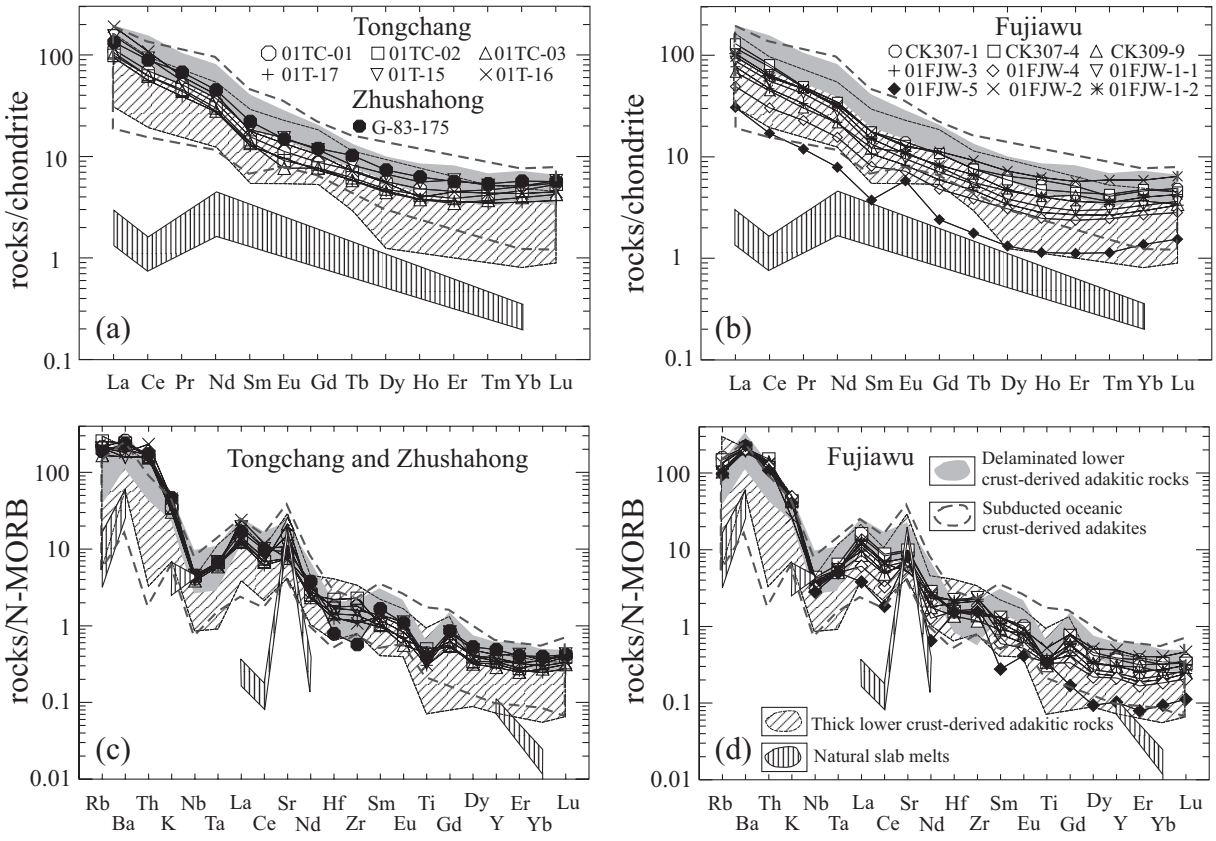

Fig. 6. Chondrite normalized rare earth element (REE) patterns and N-MORB normalized multi-element profiles of the intrusive rocks in the Dexing area. Chondrite and N-MORB normalizing values are from Boynton (1984) and Sun & McDonough (1989), respectively. (a) REE patterns of the Tongchang and Zhushahong adakitic porphyries. (b) REE patterns of the Fujiawu adakitic porphyries. (c) Multi-element profiles of the Tongchang and Zhushahong adakitic porphyries. (d) Multi-element profiles of the Fujiawu adakitic porphyries. The data for the Dexing adakitic porphyries are from Table 2. The REE and trace element data for delaminated lower crust-derived adakitic rocks, subducted oceanic crust-derived adakites, thick lower crust-derived adakitic rocks, and pure slab melts are from the same data sources as in Fig. 4.

Yangtze Block, which mainly originated from crustal melting (Fig. 8; Chen & Jahn, 1998). In summary, the Dexing adakitic porphyries have Nd isotopic signatures similar to those of mantle-derived rocks, suggesting that a significant mantle component with depleted Nd isotopic composition could be involved in their petrogenesis.

DISCUSSION

Tectonic setting

It is generally accepted that East China has been part of the Eurasian continental plate since North China and South China were joined in the Triassic (e.g. Li *et al.*, 1993). Extensive granitic and intermediate–acid volcanic rocks of Cretaceous and Jurassic age are exposed in East China (Fig. 1b). Although it has been proposed that the Late Mesozoic magmatism in southeast China may have been related to westward subduction of the paleo-Pacific plate (e.g. Xu *et al.*, 1999; Zhou & Li, 2000), there is no well-documented evidence to support the idea that there was subduction beneath South China at that time (e.g. Li *et al.*, 2003, 2004), especially in the Jurassic (Fig. 1a) (e.g. Ratschbacher *et al.*, 2000). Recently, it has been proposed that the Late Mesozoic magmatism of South China was formed in an extensional tectonic setting rather than above a subduction zone (Li *et al.*, 2003, 2004; Wang *et al.*, 2003*b*, 2004*c*). Middle Jurassic (160–180 Ma) intra-plate alkaline basalts and gabbros, bimodal volcanic–intrusive complexes (Fig. 1b; Zhao *et al.*, 2001; Li *et al.*, 2003, 2004; Wang *et al.*, 2003*b*, 2004*c*), and Jurassic extensional sedimentary basins (Gilder *et al.*, 1996) are all observed in this region. In addition, A-type granites and alkali gabbro–aegirine syenite suites with ages of 165–172 Ma have been reported (Li *et al.*, 2003). These provide strong evidence against an arc setting, as peralkaline igneous rocks have not been reported to occur in subduction-related tectonic settings. Therefore, an extensional tectonic regime in South China was possibly initiated in the Middle Jurassic (Gilder *et al.*, 1996;

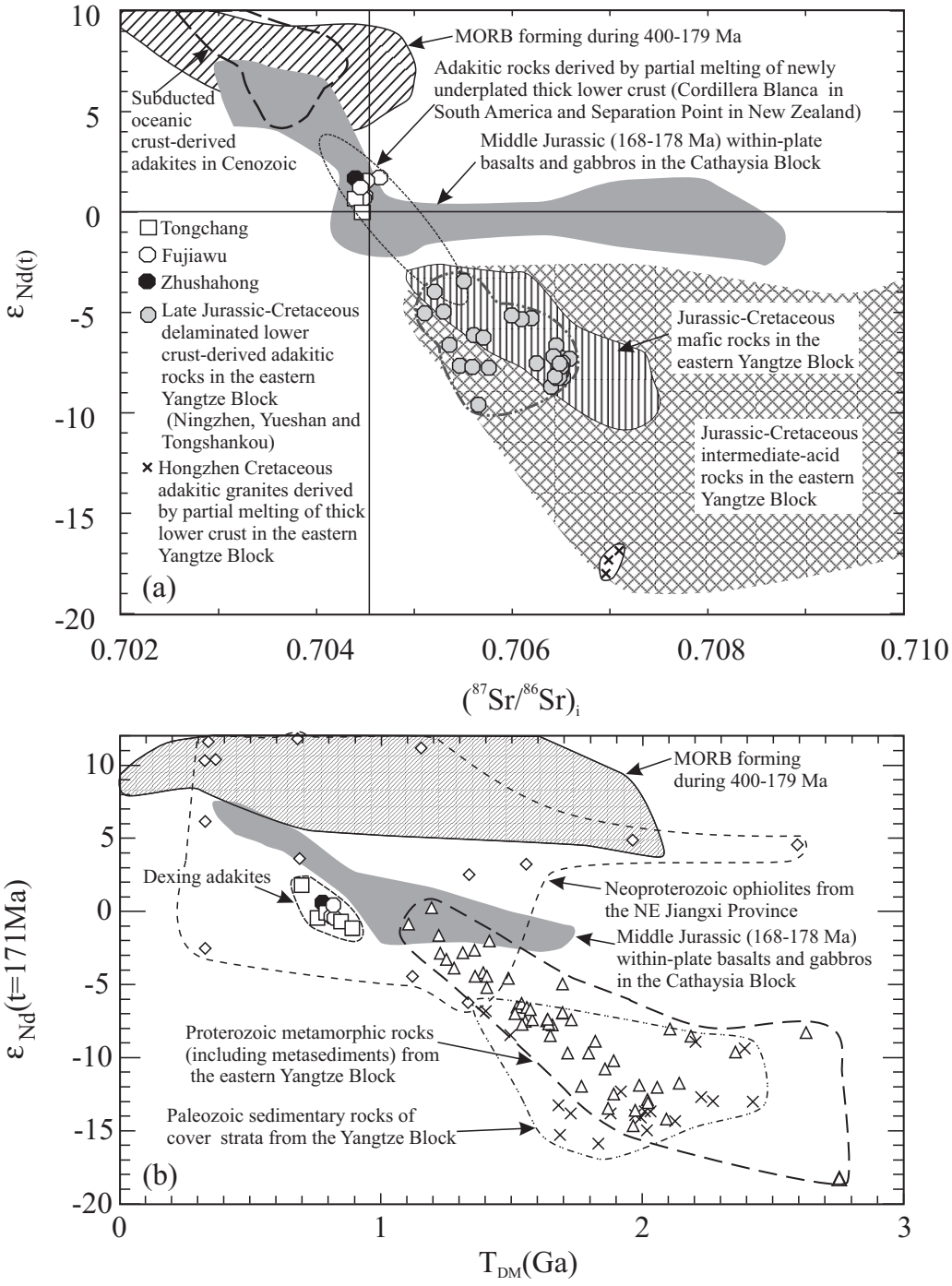

Fig. 7. (a) Nd–Sr isotope compositions of the intrusive rocks in the Dexing and adjacent areas. Data source are as follows: Dexing adakitic porphyries are from Table 3; adakitic rocks directly derived from a thick crust (lower crustal melting) are after Atherton & Petford (1993), Muir *et al.* (1995) and Petford & Atherton (1996); Cenozoic subducted oceanic crust-derived adakites are after Defant *et al.* (1992), Kay *et al.* (1993), Sajona *et al.* (2000) and Aguillón-Robles *et al.* (2001); 400–179 Ma MORB are from Mahoney *et al.* (1998), Xu *et al.* (2003), Tribuzio *et al.* (2004) and Xu & Castillo (2004); delaminated lower crust-derived adakitic rocks are from Xu *et al.* (2002) and Wang *et al.* (2004*a*, 2004*b*); the Hongzhen Cretaceous adakitic granites are from Wang *et al.* (2004*a*); Jurassic–Cretaceous mafic and intermediate–acid rocks in the eastern Yangtze Block are from Chen & Jahn (1998), Wang (2000), Xu *et al.* (2002) and Wang *et al.* (2003*a*, 2003*c*); Middle Jurassic (168–178 Ma) within-plate basalts and gabbros in the Cathaysia Block are from Li *et al.* (2003, 2004) and Wang *et al.* (2003*b*, 2004*c*). (b) Nd model age (T_{DM}) vs $\varepsilon_{Nd}(t) = 171$ Ma for the Dexing adakitic porphyries compared with Proterozoic metamorphic rocks from the Yangtze Block (Chen & Jahn, 1998), Paleozoic sedimentary rocks of cover strata from the Yangtze Block (Chen & Jahn, 1998), Proterozoic ophiolites from the northeastern Jiangxi Province (Li *et al.*, 1997), Middle Jurassic (168–178 Ma) within-plate basalts and gabbros in the Cathaysia Block and 400–179 Ma MORB.

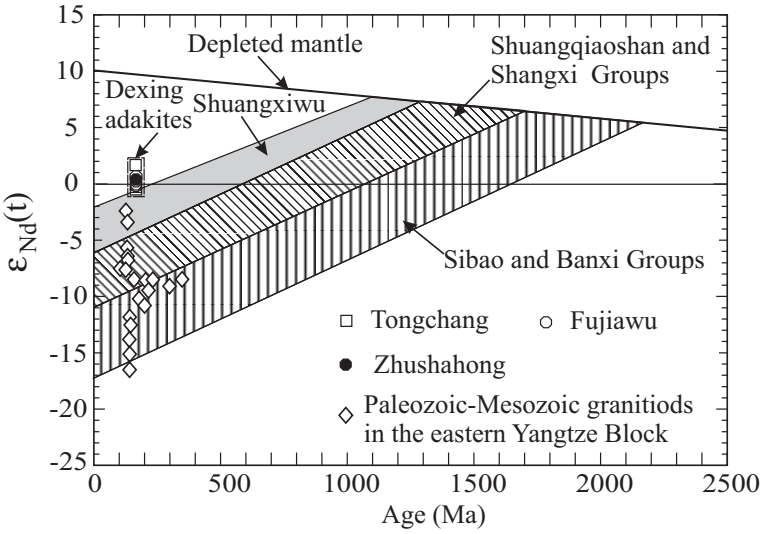

Fig. 8. Nd isotope evolution diagram for the Yangtze Block (modified from Chen & Jahn, 1998). Two major crust-forming events are represented by the Banxi–Sibao Groups (NW Yangtze, ~1800 Ma) and the Shangxi–Shuangqiaoshan Groups (SE Yangtze, ~1400 Ma). The third event is represented by the Shuangxiwu Group (~1000–875 Ma). The Proterozoic rocks appear to have played an important role in the generation of the Mesozoic igneous rocks (Chen & Jahn, 1998). Samples of the Dexing adakitic porphyries have relatively high ε_{Nd}, suggesting a significant depleted mantle component is involved in their petrogenesis.

Zhao *et al.*, 2001; Li *et al.*, 2003, 2004; Wang *et al.*, 2003*b*, 2004*c*). The Dexing porphyries were generated in the Middle Jurassic (171 ± 3 Ma), and occur near to the Middle Jurassic–Cretaceous Shi-Hang rift zone (Fig. 1b; Goodell *et al.*, 1991; Gilder *et al.*, 1996); therefore, it is reasonable to conclude that they were also emplaced in an extensional tectonic setting in the interior of the continent rather than in a subduction zone setting.

Petrogenesis of the Dexing adakitic porphyries

Several genetic models have been proposed to account for the origin of adakites and adakitic rocks. These include: (1) partial melting of a subducting oceanic slab (e.g. Defant & Drummond, 1990; Kay *et al.*, 1993; Stern & Kilian, 1996; Martin *et al.*, 2005); (2) crustal assimilation and fractional crystallization (AFC) processes from parental basaltic magmas (e.g. Castillo *et al.* 1999); (3) partial melting of mafic rocks in the lower part of a thickened crust (Atherton & Petford, 1993; Muir *et al.*, 1995; Petford & Atherton, 1996; Xiong *et al.*, 2003); (4) partial melting of a stalled (or dead) slab in the mantle (Pe-Piper & Piper, 1994; Defant *et al.*, 2002; Mungall, 2002; Qu *et al.*, 2004); (5) partial melting of delaminated lower crust (Kay & Kay, 1993; Xu *et al.*, 2002; Gao *et al.*, 2004; Wang *et al.*, 2004*a*, 2004*b*).

On the basis of the tectonic setting, geochemical characteristics, and zircon U–Pb dating the first three models appear unlikely explanations for the petrogenesis of the Dexing adakitic porphyries, whereas the latter two models seem more plausible.

Models 1–3: Slab melting, AFC process and lower crustal melting

As there is little geodynamic evidence for the existence of contemporaneous subduction, combined with the observation that the Dexing adakitic porphyries have much lower $\varepsilon_{Nd}(t)$ = 171 Ma) than those of 400–179 Ma MORB (representing appropriate subducted oceanic crustal protoliths) and Cenozoic adakites (Fig. 7), and higher Th contents and Th/Ce ratios than subducted slab-derived adakites (Fig. 5i and j), we conclude that the Dexing adakitic porphyries were unlikely to have been produced by partial melting of subducted oceanic crust in the Middle Jurassic.

The Dexing adakitic porphyries have the highest $\varepsilon_{Nd}(t)$ and lowest initial $^{87}Sr/^{86}Sr$ ratios of the Late Mesozoic magmatic rocks of the eastern Yangtze Block, including mafic rocks (Figs 7a and 8), indicating that they could not have been generated through an AFC process from contemporaneous mafic magmas. Although the samples of the Dexing porphyries could be interpreted as showing a slight fractional crystallization trend in a plot of La/Yb vs Yb (Fig. 9a), the data are more consistent with a partial melting trend (Fig. 9a), suggesting that the effects of source partial melting were more important than fractional crystallization in controlling the compositional variation within the Dexing adakitic porphyries. A plot of the compatible element Ni vs the incompatible element Th (Fig. 9b) further supports that the suggestion that fractional crystallization could not have produced the geochemical variation within the Dexing adakitic porphyries. Moreover, the lack of inherited zircons (Fig. 2)

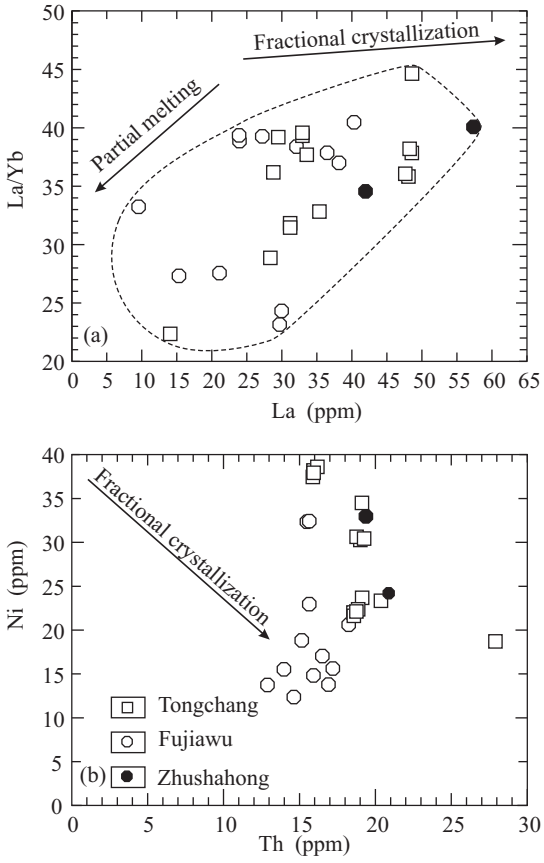

Fig. 9. La/Yb vs La (a) and Ni vs Th (b) diagram for the Dexing adakite porphyries.

and relatively high Mg-number ((100 × Mg^{2+}/(Mg^{2+} + Fe^{total})) = 47–60) (Fig. 10a) of the Dexing adakitic porphyries clearly indicates that they were probably not generated from a parental basaltic magma which assimilated old crustal material and concurrently underwent fractional crystallization (Castillo *et al.*, 1999).

The Nd–Sr isotopic compositions of the Dexing adakites, which are comparable with those of coeval basaltic magmas from the Cathaysia Block (Li *et al.*, 2003, 2004; Wang *et al.*, 2003*b*, 2004*c*) and to those of adakitic rocks derived by partial melting of newly underplated basaltic lower crust (Atherton & Petford, 1993; Muir *et al.*, 1995; Petford & Atherton, 1996; Fig. 7a), invite speculation that they may have occurred due to partial melting of newly underplated, thickened, lower crust. Nevertheless, most samples of the Dexing adakitic porphyries have higher MgO (or Mg-number), Cr and Ni, but lower FeO^T/MgO and Al_2O_3 contents, relative to adakitic rocks derived by this process (Figs 5c–g and 10), suggesting that they were unlikely to have been derived by partial melting of underplated basaltic rocks during the Middle Jurassic. In addition, the source of the Dexing adakitic porphyries clearly contains a significant mantle component with a depleted Nd isotopic composition (Figs 7 and 8); this is different from that of the lower crust-derived adakitic rocks in the eastern Yangtze Block (e.g. the Hongzhen adakitic rocks; Fig. 7a).

Model 4: Partial melting of a Neoproterozoic stalled slab

To the east of the Dexing adakitic porphyries (Fig. 1c), there is a suite of Neoproterozoic (~1000 Ma) ophiolitic melanges that occur as discrete lenses along the Yiyang–Dexing fault zone (Chen *et al.*, 1991; Li *et al.*, 1997). The Dexing adakitic porphyries have Nd isotopic compositions similar to those (at T = 171 Ma) of the ophiolites (Fig. 7b), suggesting that they could be derived by partial melting of the remnants of a Neoproterozoic subducted slab, stalled in the mantle. If these adakitic magmas were generated by partial melting of such a stalled slab, then it is possible that they interacted with the mantle during ascent, and as a consequence they exhibit higher MgO (or Mg-number), Cr, Ni and Yb (Figs 5e–h and 10) but slightly lower FeO^T/MgO and Al_2O_3 (Fig. 5c and d) relative to experimental melts of basaltic rocks (Sen & Dunn, 1994; Rapp *et al.*, 1991, 1999, 2002, 2003; Rapp & Watson, 1995; Prouteau *et al.*, 1999; Skjerlie & Patiño Douce, 2002, and references therein), and pure slab melts (Sorensen & Grossman, 1989; Kepezhinskas *et al.*, 1995) (Mg-number < 47). However, it must be noted that the Dexing adakitic porphyries have distinctly higher Th contents and Th/Ce ratios than subducted slab-derived adakites (Fig. 5i and j), which weakens the possibility that they originated from a stalled slab. Moreover, it is questionable whether the Neoproterozoic subducted slab could have stayed in the mantle until the Middle Jurassic without being subjected to melting, because after the Neoproterozoic (1000–900 Ma) collision between the Yangtze and Cathaysia Blocks, South China went through a complex tectonic evolution from the Neoproterozoic to the early Jurassic, including mantle superplume activities at 860–750 Ma (Li *et al.*, 2002*a*, 2002*b*). Moreover, any slab subducted into the convecting mantle would have sunk to the bottom of the upper (or even lower) mantle quite rapidly; additionally, the lithosphere itself will have moved significantly since 1000 Ma and it seems impossible that it could still be sitting above the same part of the convecting mantle in the Jurassic. Accordingly, it is still difficult to interpret the Dexing adakitic porphyries as partial melts of a subducted slab stalled in mantle, although we cannot completely rule out this possibility.

Model 5: Partial melting of delaminated lower crust

The Dexing adakitic porphyries are similar to the adakites derived from subducted oceanic crust (Defant & Drummond, 1990; Kay *et al.*, 1993; Drummond *et al.*,

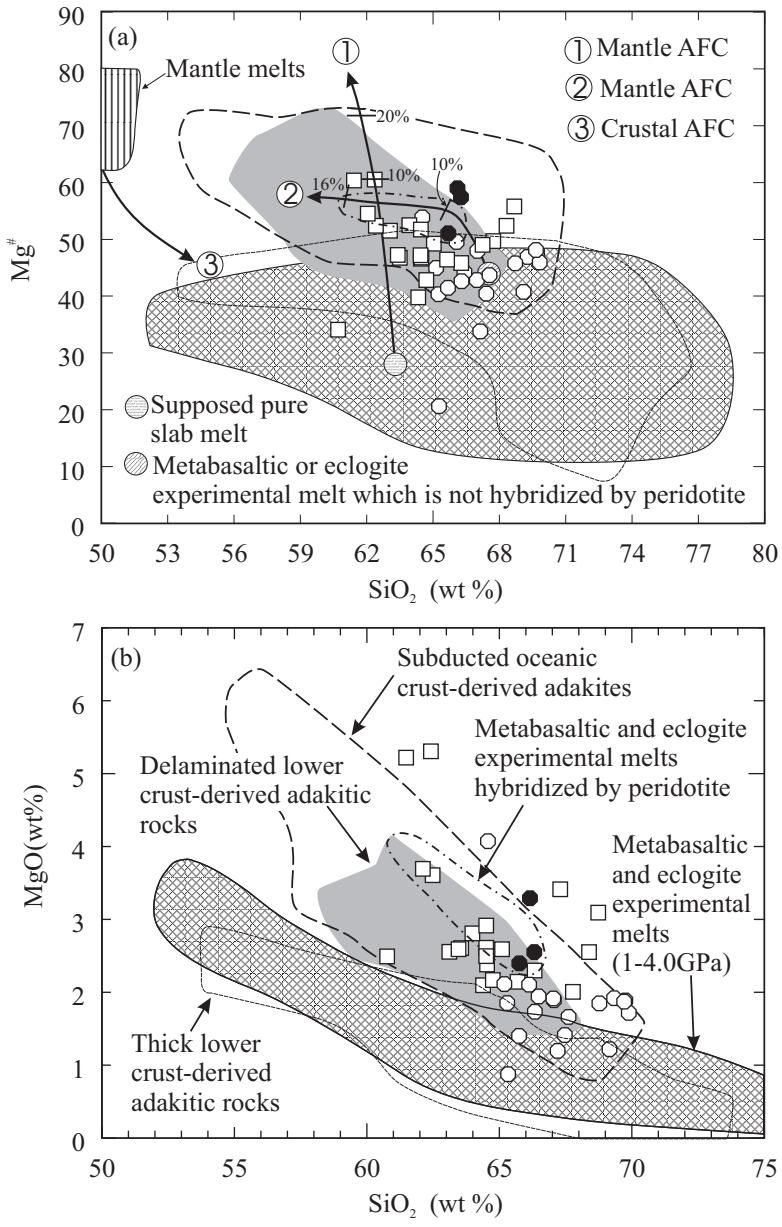

Fig. 10. Mg-number (a) and MgO wt % (b) vs SiO_2 (wt %) diagrams for the Dexing adakitic porphyries. Mantle AFC curves are after Stern & Killian (1996) (Curve 1) and Rapp *et al.* (1999) (Curve 2); the proportion of assimilated peridotite is also shown. The crustal AFC curve is after Stern & Killian (1996) (Curve 3). The starting point of Curve 1 represents the composition of a pure slab melt, which is supposed by Stern & Killian (1996). The starting point of Curve 2 represents the composition of a metabasaltic or eclogite experimental melt, which is not hybridized with peridotite (Rapp *et al.*, 1999). Fields of delaminated lower crust-derived adakitic rocks, subducted oceanic crust-derived adakites and thick lower crust-derived adakitic rocks are constructed using the same data sources as those in Fig. 4. The field of metabasaltic and eclogite experimental melts (1–4·0 GPa) is from the following: Rapp *et al.* (1991, 1999, 2002); Sen & Dunn (1994); Rapp & Watson (1995); Prouteau *et al.* (1999); Skjerlie & Patiño Douce (2002), and references therein. The field of metabasaltic and eclogite experimental melts hybridized with peridotite is after Rapp *et al.* (1999).

1996; Kepezhinskas *et al.*, 1995; Stern & Kilian, 1996; Aguillón-Robles *et al.*, 2001; Defant *et al.* 2002; Bourdon *et al.*, 2002), adakitic rocks derived from delaminated lower crust (Xu *et al.*, 2002; Wang *et al.*, 2004*a*, 2004*b*) and metabasaltic and eclogite experimental melts hybridized by peridotite (Rapp *et al.*, 1999) in terms of their FeO^T/MgO, Al_2O_3, MgO (or Mg-number) and Cr, Ni and Yb contents (Figs 5c–h and 10). It is generally believed that reaction between pure slab melts and surrounding peridotite in the sub-arc mantle wedge (e.g. Kepezhinskas *et al.*, 1995; Stern & Kilian, 1996; Rapp *et al.*, 1999; Smithies, 2000) results in the high

Mg-number and MgO contents of adakites (Fig. 10). In addition, the Nd–Sr isotopic signatures of the Dexing adakitic porphyries also confirm that a mantle component probably played a role in their petrogenesis (Figs 7 and 8). The relatively high SiO_2 (60–70%) contents of the Dexing adakitic porphyries (Fig. 4a; Table 2) indicate that they could not be directly generated by partial melting of mantle peridotite because low degree partial melting of mantle peridotite can yield melts only as silicic as basaltic andesite, or boninite rather than dacite in composition (Green, 1980; Jahn & Zhang, 1984). Experimental results (Baker *et al.*, 1995) for partial melting of anhydrous lherzolite also show that liquid compositions are not more silicic than andesite (~55% SiO_2) even at melt fractions as low as 2%. Therefore, the Dexing adakitic porphyries were unlikely to have been produced by partial melting of anhydrous mantle peridotite. Additionally, the high Th contents and Th/Ce ratios of the Dexing adakitic porphyries (Fig. 5i and j) indicate that their source was probably of lower continental crustal origin (Hawkesworth *et al.*, 1997; Rapp *et al.*, 2002; Wang *et al.*, 2005). Therefore, the most probable scenario that can explain the elevated MgO, Mg-number, Cr, Ni, Yb and Th contents, but low Al_2O_3 and FeO^T/MgO, of the Dexing adakitic porphyries is partial melting of lower crust during delamination, similar to the model proposed for the Late Jurassic–Cretaceous Ningzhen, Yueshan and Tongshankou adakitic intrusive rocks in the eastern Yangtze Block (Xu *et al.*, 2002; Wang *et al.*, 2004*a*, 2004*b*). In this case, the delaminated section of the lower crust is heated by the surrounding relatively hot mantle and undergoes partial melting (e.g. Kay & Kay, 1993). The resultant melt rises through a zone of mantle peridotite *en route* to its emplacement in the upper crust, with significant chemical interaction between the mantle peridotite and the crustal melt (Fig. 10).

The oldest rocks exposed in the Dexing and adjacent areas are Proterozoic in age (Fig. 1c). These include metamorphic, arc volcanic and sedimentary rocks, and ophiolites. Except for some ophiolites and metamorphic rocks which have $\varepsilon_{Nd}(t)$ values at 171 Ma close to those of the Dexing adakitic porphyries (Figs 7b and 8), the majority of the local lower crustal rocks have lower $\varepsilon_{Nd}(171\ Ma)$ than those of the adakites. The Nd isotopic compositions of the metamorphic arc volcanic rocks and metasediments of the Shuangxiwu Group (Fig. 8) are the closest to those of the Dexing adakitic porphyries. On the assumption that the initial adakitic magmas derived by partial melting of such delaminated lower crustal rocks and subsequently interacted with the overlying mantle during their ascent, the effect would be to increase the $\varepsilon_{Nd}(171\ Ma)$ of the resulting adakitic magmas (Figs 7b and 8). Consequently, it is possible that partial melting of delaminated lower crust could have generated the Dexing adakitic rocks; the amount of interaction with the surrounding mantle would directly correlate with the $\varepsilon_{Nd}(171\ Ma)$ of the lower crust.

Geodynamic model for generating the Dexing adakitic porphyries

As mentioned above, the most probable petrogenetic model for generating the Dexing adakitic magmas is partial melting of delaminated lower crust during the late Mesozoic. We now consider possible geodynamic scenarios that might lead to delamination and partial melting of the lower crust in the Jurassic.

Lower crustal delamination may represent an important process in the differentiation of the continental lithosphere (Ducea & Saleeby, 1998). In the west of both North and South America, lower crustal delamination has been suggested on the basis of xenolith studies, magmatism and geophysical evidence (Kay & Kay, 1993; Ducea & Saleeby, 1998; Zandt *et al.*, 2004). Xu *et al.* (2002) also concluded that the Cretaceous adakitic intrusive rocks in the Yangtze block were derived from delaminated lower crust. Experimental studies (e.g. Rapp & Watson, 1995; Rapp *et al.*, 1999, 2002, 2003) have also shown that mafic crustal rocks can melt to produce adakitic liquids at sufficient depths (>40 km, i.e. ~1·2 GPa) for garnet to be stable within the residual assemblage (e.g. residues of garnet-amphibolite, amphibole-bearing eclogite and/or eclogite). The Dexing adakitic porphyries exhibit the typical geochemical characteristics of adakites, e.g. high La/Yb, Sr/Y ratios and low Y and Yb contents (Table 2; Figs 4b and 6), suggesting that garnet was stable within the source residues when the adakitic magmas were segregated (Defant & Drummond, 1990; Atherton & Petford, 1993; Rapp & Watson, 1995; Rapp *et al.*, 1999, 2003). Consequently, the crustal thickness in the Dexing area must have been at least 40 km when the adakitic porphyries were formed in the Middle Jurassic. However, the present crustal thickness in the Dexing area is only ~31 km (Fig. 11; Wang, 1992; Ma *et al.*, 1994; Tang *et al.*, 1998). This implies that the continental crust in the Dexing area has undergone some thinning since the Mesozoic. As effusive rhyolites and tuffs of the late Jurassic Ehu formation are still preserved in the Dexing area (Fig. 1d), the ~10 km thick upper crust cannot have been thinned by surface erosion since the formation of the adakitic rocks. Notwithstanding the fact that Late Mesozoic–present lithospheric extension (including the formation of metamorphic core complexes) also caused crustal thinning in southeastern China (Ratschbacher *et al.*, 2000; Wang *et al.*, 2004*a*), we believe that delamination mainly resulted in the thinning of the crust during the Mesozoic in the Dexing area as a consequence of sinking of eclogitic material from the base of the crust into the underlying mantle (Fig. 12). As the continental crust at this time was probably

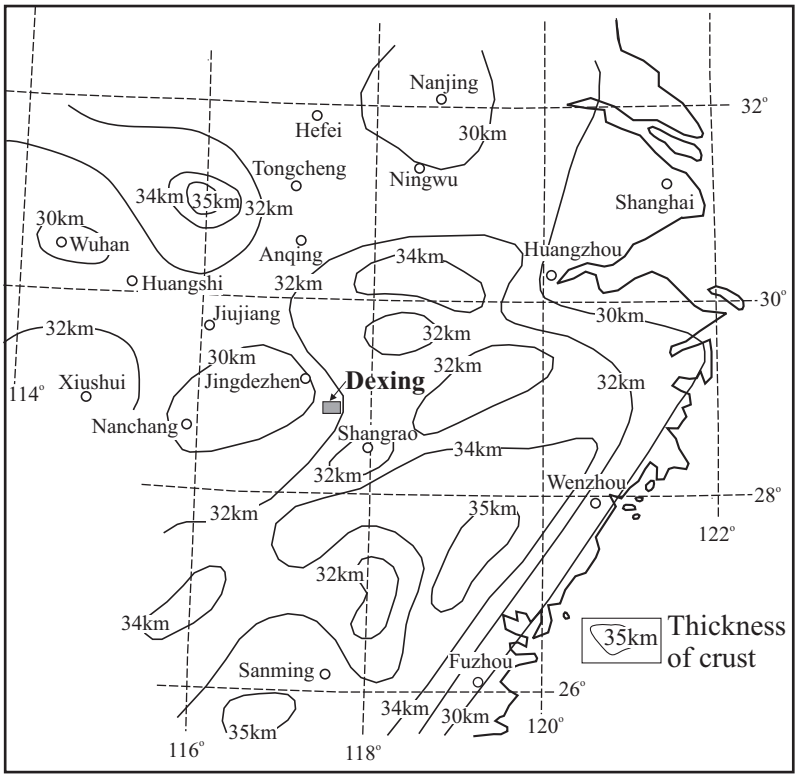

Fig. 11. Contour map of present-day crustal thickness (km) in Southeast China (after Wang (1992); Ma *et al.* (1994); Tang *et al.* (1998)).

over-thickened, as a consequence of Triassic compression in South China (e.g. Chen, 1999; Li *et al.*, 2003, 2004), the increase in pressure and temperature might have converted mafic rocks in the lower crust into amphibole-bearing eclogites. The high density of such garnet-bearing mafic rocks in the lower crust leads to delamination (Kay & Kay, 1993; Ducea & Saleeby, 1998; Xu *et al.*, 2002; Wang *et al.*, 2004*a*, 2004*b*) or foundering (Arndt & Goldstein, 1989; Ducea & Saleeby, 1998; Gao *et al.*, 2004; Zandt *et al.*, 2004).

Partial melting of the delaminated lower crust might have been triggered by the Middle Jurassic extension of the Shi–Hang rift. Rifting initiated in the Middle Jurassic (Gilder *et al.*, 1996; Wang *et al.*, 2003*b*, 2004*c*; Li *et al.*, 2004), and might have led to the upwelling of hotter asthenospheric mantle along deep fault zones (e.g. the Yiyang–Dexing fault) (Fig. 12). As a consequence, conduction of heat from the underlying asthenosphere heated both the lithospheric mantle and the source (delaminated lower crust) of the Dexing adakitic porphyries (Fig. 12b). As noted above, in addition to garnet, their source is also inferred to have contained residual amphibole, as indicated by the concave MREE patterns of the adakites (Fig. 6 a and b). We consider that the flux of heat from the underlying asthenosphere triggered dehydration partial melting of delaminated lower crust (amphibole-bearing eclogite) in the lithospheric mantle; the resulting magmas then reacted with the surrounding mantle peridotite to form the Dexing adakitic porphyries (Fig. 12b).

Implications for genesis of porphyry copper deposits

Porphyry copper deposits are generally derived from sulfur-rich, highly oxidized magmatic systems, with oxygen fugacities (fO_2) between the nickel–nickel oxide (NNO) or sulfide–sulfur oxide (SSO) and magnetite–hematite oxygen (MH) buffers (Imai *et al.*, 1993; Sillitoe, 1997; Oyarzún *et al.*, 2001; Mungall, 2002). The chalcophile elements are mainly stored in mantle sulfides (e.g. Sillitoe, 1997; Mungall, 2002). The transport of chalcophile elements from the mantle by magmas will occur if sulfide phases are completely consumed during partial melting; this requires the oxidation state of the mantle to be up to values of log fO_2 > FMQ (fayalite–magnetite–quartz oxygen buffer) + 2 (i.e. higher than the SSO buffer; e.g. Mungall, 2002). The upper part of subducted oceanic crust has a very high intrinsic fO_2 due to equilibration with seawater during hydrothermal alteration and deposition of terrigenous sediment (e.g. McInnes & Cameron, 1994; Mungall, 2002). Melts or

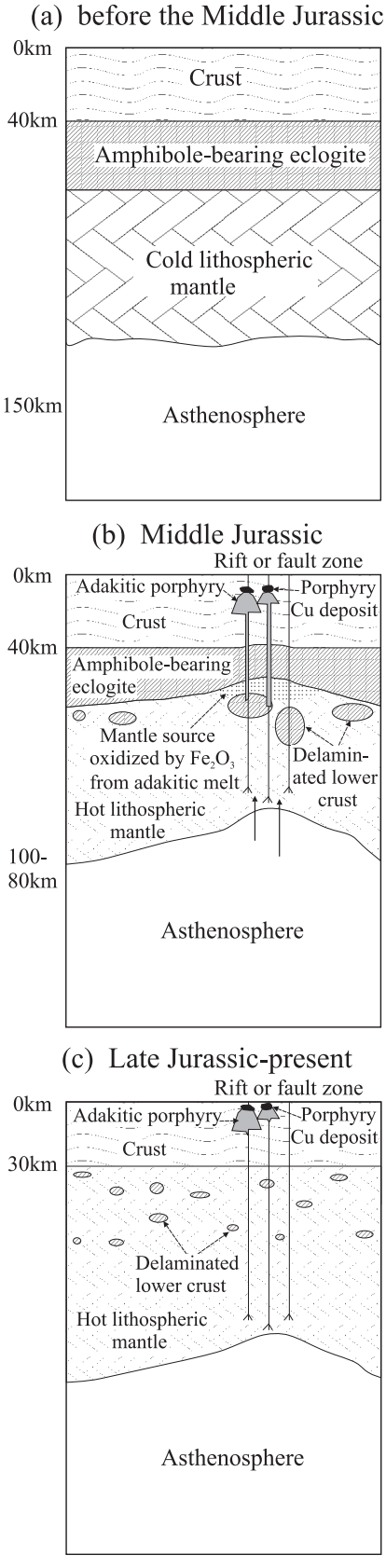

fluid derived from the slab will carry this oxidizing potential up into the overlying mantle and destabilize mantle sulfides to release Cu and Au (McInnes & Cameron, 1994; Sillitoe, 1997; Mungall, 2002). Slab-derived adakitic magmas are more favorable for the generation of Cu–Au deposits than slab-derived CO_2- or H_2O- or SO_3-bearing fluids, owing to their higher Fe_2O_3 content (Mungall, 2002). Therefore, adakites derived by slab melting have been recognized as being particularly effective agents of Cu–Au mineralization (Thiéblemont *et al.*, 1997; Oyarzún, *et al.*, 2001; Defant *et al.*, 2002; Mungall, 2002) and, consequently, have been regarded as important indicators in gold and copper exploration (Defant *et al.*, 2002). Favorable tectonic settings for the generation of porphyry Cu–Au deposits associated with slab melting are subduction of very young lithosphere or very slow or oblique convergence, flat subduction, and the presence of a dead or stalled slab (Sillitoe, 1997; Mungall, 2002).

Mungall (2002) proposed that only slab-derived adakitic magmas or supercritical fluids would have a sufficiently high oxidation potential to generate epithermal and porphyry Cu–Au deposits, and, conversely, that adakitic magmas derived by melting of underplated basaltic or gabbroic rocks in the lower crust would retain the low fO_2 of their source and not be favorable for the generation of Cu–Au deposits. In addition to fO_2, we suggest that another important factor that controls Cu–Au mineralization is the source of the chalcophile elements. As the adakitic magmas directly derived by partial melting of a thick lower crustal source do not subsequently pass through mantle rocks, in which the chalcophile elements are mainly stored, they rarely have the potential to generate Cu–Au mineralization. For example, in the eastern Yangtze Block, the Hongzhen adakitic rocks, which are considered to be directly produced by partial melting of thick lower crust, are barren of Cu–Au mineralization (Fig. 1b; Wang *et al.*, 2004*a*), whereas the delaminated

Fig. 12. A suggested model to produce the Dexing adakitic porphyries via partial melting of delaminated lower crust in the Middle Jurassic. (a) The relatively cold lithosphere and thick crust before the Middle Jurassic. The lower portion of the thick crust is composed of amphibole-bearing eclogite. (b) The hot asthenospheric mantle rises along the deep fault zone (e.g. the Yiyang–Dexing deep fault zone) due to extension of the Shi–Hang rift zone in the Middle Jurassic (Gilder *et al.* (1996)); at the same time, the thick lower crust is removed through delamination. The delaminated lower crust begins to partially melt when it sinks into the underlying mantle. The adakitic melts are produced by partial melting of delaminated lower crust, which is heated by the surrounding relatively hot mantle, coupled with the flux of heat from the upwelling asthenosphere. The adakitic melts react with the surrounding mantle peridotite, elevating their MgO, Cr and Ni contents but reducing their FeO^T/MgO ratios. At the same time, the fO_2 of the surrounding mantle may have become elevated. The metallic sulfides in the mantle are oxidized, which causes the chalcophile elements to enter the adakitic magma. (c) Late Jurassic–present, accompanying lower crustal delamination, surface erosion, and lithospheric or crustal extension result in the present-day thinned crust.

lower crust-derived Ningzhen, Yueshan and Tongshankou adakitic rocks are associated with epithermal-porphyry Cu deposits (Tang *et al.*, 1998; Xu *et al.*, 2002; Wang *et al.*, 2004*a*, 2004*b*).

We suggest that the mantle source of the chalcophile elements plays a crucial role in the Cu mineralization of the Dexing area, as supported by following evidence.

(1) The Re–Os age (~173 Ma) of molybdenite from the Dexing porphyry Cu deposits (Mao & Wang, 2000) is identical to the SHRIMP zircon U–Pb age (171 ± 3 Ma) of the Tongchang and Fujiawu adakitic porphyries, supporting the notion that the porphyry Cu deposits are related to the formation of the adakitic porphyries.
(2) The $\delta^{34}S$ values of sulfide and sulfate from the Dexing porphyry Cu deposits range from −4·0 to +3·1‰, with an average value of +0·12‰ (Zhu *et al.*, 1983; Rui *et al.*, 1984). This value is very close to that of chondrites (0–0·7‰), suggesting that the sulfur was mainly derived from a mantle source.
(3) The Dexing porphyry Cu deposit was formed under high fO_2 conditions. The adakitic porphyries contain abundant primary magnetite, hematite and anhydrite in equilibrium with hypogene copper–iron sulfide minerals (e.g. chalcopyrite and bornite) (Zhu *et al.*, 1983; Rui *et al.*, 1984). In addition, the adakitic porphyries are similar to highly oxidized I-type or magnetite-series granitoids (Zhu *et al.*, 1983; Rui *et al.*, 1984). Fe^{3+}/Fe^{2+} ratios in biotites from the adakitic porphyries plot in the field between the NNO (or SSO) and magnetite–hematite oxygen (MH) buffers in an Fe^{3+}–Fe^{2+}–Mg diagram (fig. 5.8 of Rui *et al.* (1984)). As mentioned above, provided that the Middle Jurassic lower crust in the Dexing area was composed of metamorphic arc volcanic and sedimentary rocks of the Shuangxiwu Group (Fig. 8), it could have a high oxidation potential which would be inherited by the resultant adakitic magmas.

During partial melting of delaminated lower crust in the middle Jurassic (Fig. 12b), adakitic magmas with high Fe_2O_3 contents interacted with the surrounding mantle peridotite, increasing the oxidation state of the mantle to beyond the SSO buffer, causing metallic sulfides in the mantle to be consumed (Mungall, 2002). Following the same calculation as for adakitic magma derived from slab melting (Mungall, 2002), it is found that 1 g of adakitic melt derived from partial melting of delaminated lower crust could oxidize the same amount of sulfide contained in 160 g of mantle peridotite as an adakitic magma derived from slab melting. Accordingly, we strongly suggest that adakitic magmas derived by partial melting of delaminated lower crust could be just as favorable for the generation of porphyry Cu–Au deposits (Fig. 12) as slab-derived adakitic magmas.

CONCLUSIONS

(1) Middle Jurassic (171 ± 3 Ma) adakitic porphyries and associated porphyry copper deposits in the Dexing area were generated in an extensional tectonic regime in the interior of a continent, rather than in an arc setting.
(2) The Dexing adakitic porphyries were probably derived from dehydration melting of delaminated mafic lower crust in the mantle at pressures greater than 1·2 GPa, leaving residual garnet ± amphibole in their source.
(3) High Th contents and Th/Ce ratios indicate that the Dexing adakitic magmas include a lower continental crustal component. However, their high MgO, Cr and Ni contents as well as low initial $^{87}Sr/^{86}Sr$ and FeO^T/MgO values and high εNd(t) values suggest that the adakitic magmas include a significant mantle component, contributed by interaction between the crustal melts and the surrounding mantle peridotite.
(4) The metallogenesis of the Dexing porphyry Cu deposits is intimately related to the petrogenesis of the adakites, indicating that an adakitic magma derived from delaminated lower crust also has the potential to generate porphyry Cu–Au deposits similar to slab-derived adakitic magmas.

ACKNOWLEDGEMENTS

We sincerely thank Professor Marjorie Wilson, Drs R. P. Rapp and P. R Castillo, and an anonymous reviewer for their constructive reviews and help in correcting problems with the English in the original manuscript. Dr Marc J. Defant is gratefully acknowledged for making very valuable comments on an earlier version of this paper. We are grateful to Dr Derek Wyman for helpful discussion. Professor Liu Dunyi, Tao Hua, Zhang Yuhai, Sun Xingya, Dai Youfang, Liu Ying, Hu Guangqian and Chen Zhenyu are thanked for their assistance with laboratory and fieldwork. Financial support for this research was provided by the National Natural Science Foundation of China (Grant No. 40273019, 40421303, 40425003), the Knowledge Innovation Program of the Chinese Academy of Sciences (KZCX3-SW-122, A15-041107, KZCX2-SW-117) and the Major State Basic Research Program of People's Republic of China (No. 2002CB412601).

REFERENCES

Aguillón-Robles, A., Caimus, T., Bellon, H., Maury, R. C., Cotton, J., Bourgois, J. & Michaud, F. (2001). Late Miocene adakites and Nb-enriched basalts from Vizcaino Peninsula, Mexico: indicators of

East Pacific Rise subduction below southern Baja California. *Geology* **29**, 531–534.

Arculus, R. J. (2003). Use and abuse of the terms calcalkaline and calcalkalic. *Journal of Petrology* **44**, 929–935.

Arculus, R. J., Lapierrre, H. & Jaillard, E. (1999). Geochemical window into subduction and accretion processes: Raspas metamorphic complex, Ecuador. *Geology* **27**, 547–550.

Arndt, N. T. & Goldstein, S. L. (1989). An open boundary between lower continental crust and mantle: Its role in crust. *Tectonophysics* **161**, 201–212.

Atherton, M. P. & Petford, N. (1993). Generation of sodium-rich magmas from newly underplated basaltic crust. *Nature* **362**, 144–146.

Baker, M. B., Hischmann, M. M., Ghiorso, M. S. & Stolper, E. M. (1995). Compositions of near-solidus peridotite melts from experiments and thermodynamic calculations. *Nature* **375**, 308–311.

Bissig, T., Clark, A. H. & Lee, J. K. W. (2003). Petrogenetic and metallogenetic responses to Miocene slab flattening: New constraints from the El Indio–Pascua Au–Ag–Cu belt, Chile/Argentina. *Mineralium Deposita* **38**, 844–862.

Bourdon, E., Eissen, J. P., Monzier, M., Robin, C., Martin, H., Cotton, J. & Hall, M. L. (2002). Adakite-like lavas from Antisana volcano (Ecuador): evidence for slab melt metasomatism beneath the Andean Northern Volcanic Zone. *Journal of Petrology* **43**, 199–217.

Boynton, W. V. (1984). Cosmochemistry of the earth elements: meteorite studies. In: Henderson, R. (ed.) *Rare Earth Element Geochmistry: Developments in Geochemistry 2*, Amsterdam: Elsevier, pp. 89–92.

Castillo, P. R., Janney, P. E. & Solidum, R. U. (1999). Petrology and geochemistry of Camiguin island, southern Philippines: insights to the source of adakites and other lavas in a complex arc setting. *Contributions to Mineralogy and Petrology* **134**, 33–51.

Chen, A. (1999). Mirror thrusting in the south China orogenic belt: tectonic evidence from western Fujian, southeastern China. *Tectonophysics* **305**, 497–519.

Chen, J. F. & Jahn, B. M. (1998). Crustal evolution of Southeast China: Nd and Sr isotopic evidence. *Tectonophysics* **284**, 101–133.

Chen, J. F., Foland, K. A., Xing, F. M., Xu, X. & Zhou, T. X. (1991). Magmatism along the southeast margin of the Yangtze block: Precambrian collision of the Yangtze and Cathaysia block of China. *Geology* **19**, 815–818.

Chung, S. L., Lo, C. H., Lan, C. Y., Wang, P.L., Lee, T.Y., Joa, T.T., *et al.* (1999). Collision between the Indochina and South China blocks in the early Triassic: implications for the Indosinian Orogeny and closure of eastern paleo-Tethys. *EOS Transactions, American Geophysical Union* **80**, 1043.

Chung, S. L., Liu, D. Y., Ji, J. Q., Chu, M. F., Lee, H. Y., Wen, D. J., *et al.* (2003). Adakites from continental collision zones: melting of thickened lower crust beneath southern Tibet. *Geology* **31**, 1021–1024.

Defant, M. J. & Drummond, M. S. (1990). Derivation of some modern arc magmas by melting of young subducted lithosphere. *Nature* **347**, 662–665.

Defant, M. J., Jackson, T. E., Drummond, M. S., De Boer, J. Z., Bellon, H., Feigenson, M.D., *et al.* (1992). The geochemistry of young volcanism throughout western Panama and southeastern Costa Rica: an overview. *Journal of the Geological Society, London* **149**, 569–579.

Defant M. J., Xu J. F., Kepezhinskas, P., Wang, Q., Zhang, Q. & Xiao, L. (2002). Adakites: some variations on a theme. *Acta Petrologica Sinica* **18**, 129–142.

Drummond, M. S., Defant, M. J. & Kepezhinskas, P. K. (1996). The petrogenesis of slab derived trondhjemite–tonalite–dacite/adakite magmas. *Transactions of the Royal Society of Edinburgh–Earth Sciences* **87**, 205–216.

Ducea, M. & Saleeby, J. (1998). Crustal recycling beneath continental arcs: silica-rich glass inclusions in ultramafic xenoliths from the Sierra Nevada, California. *Earth and Planetary Science Letters* **156**, 101–116.

Gao, S., Zhang, B., Gu, X., Xie, X., Gao, C. & Guo, X. (1995). Silurian–Devonian provenance changes of South Qinling Basin: implications for accretion of the Yangtze (South China) to the North China Craton. *Tectonophysics* **250**, 183–197.

Gao, S., Rudnick, R. L., Yuan, H. L., Liu, X. M., Liu, Y. S., Xu, W. L., *et al.* (2004). Recycling lower continental crust in the North China craton. *Nature* **432**, 892–897.

Gilder, S. A., Gill, J., Coe, R. S., Zhao, X., Liu, Z., Wang, G., *et al.* (1996). Isotopic and paleomagnetic constraints on the Mesozoic tectonic evolution of south China. *Journal of Geophysical Research* **101**, 16137–16154.

Goodell, P. C., Gilder, S. & Fang, X. H. (1991). A preliminary description of the Gan–Hang failed rift, southeastern China. *Tectonophysics* **197**, 245–255.

Green, T. H. (1980). Island arc and continent-building magmatism: a review of petrogenetic models based on experimental petrology and geochemistry. *Tectonophysics* **63**, 367–385.

Gromet, L. P. & Silver, L. (1987). REE variations across the Peninsular Ranges Batholith: implications for batholithic petrogenesis and crustal growth in magmatic arcs. *Journal of Petrology* **28**, 75–125.

Gutscher, M. A., Maury, R., Eissen, J. & Bourdon, E. (2000). Can slab melting be caused by flat subduction? *Geology* **28**, 535–538.

Hawkesworth, C. J., Turner, S.P., McDermott, F., Peate, D. W. & van Calsteren, P. (1997). U–Th isotopes in arc magmas: implications for element transfer from subducted crust. *Science* **276**, 561–555.

He, W. W., Bao, Z. Y. & Li, T. P. (1999). One-dimensional reactive transport models of alteration in the Tongchang porphyry copper deposit, Dexing district, Jiangxi Province, China. *Economic Geology* **94**, 307–321.

Hollings, P. & Kerrich, R. (2000). An Archean arc basalt–Nb-enriched basalt–adakite association: the 2·7 Ga Confederation assemblage of the Birch–Uchi greenstone belt, Superior Province. *Contributions to Mineralogy and Petrology* **139**, 208–226.

Hou, Z. Q., Gao, Y. F., Qu, X. M., Rui, Z. Y. & Mo, X. X. (2004). Origin of adakitic intrusives generated during mid-Miocene east–west extension in southern Tibet. *Earth and Planetary Science Letters* **220**, 139–155.

Hua, R. M. & Dong, Z. Q. (1984). Characteristics and petrogenesis discussion of two series granitoids in the Dexing area. In: Xu, K. Q. & Tu, G. C. (eds) *The Granite Geology and the Relationship Related to Metallogenesis*. Nanjing: Jiangsu Science Press, pp. 226–240 (in Chinese).

Imai, A., Listanco, E. L. & Fujii, T. (1993). Petrologic and sulfur isotopic significance of highly oxidized and sulfur-rich magma of Mt. Pinatubo, Philippines. *Geology* **21**, 585–588.

Jahn, B. M. & Zhang, J. Q. (1984). Archean granulite gneisses from eastern Sino-Korean Province, China: rare earth geochemistry and tectonic implication. *Contributions to Mineralogy and Petrology* **85**, 224–243.

Jian, P., Liu, D. Y. & Sun, X. M. (2003). SHRIMP dating of Carboniferous Jinshajiang ophiolite in western Yunnan and Sichuan: geochronological constraints on the evolution of the Paleo-Tethys oceanic crust. *Acta Geologica Sinica* **77**, 217–277 (in Chinese with English abstract).

Jin, Z. D., Zhu, J. C. & Li, F. C. (2002). O, Sr and Nd isotopic tracing of the ore-forming process in Dexing porphyry copper deposit,

Jiangxi Province. *Mineral Deposits* **21**, 341–349 (in Chinese with English abstract).

Johnson, K., Barnes, C. G. & Miller, C. A. (1997). Petrology, geochemistry, and genesis of high-Al tonalite and trondhjemites of the Cornucopia stock, Blue Mountains, Northeastern Oregon. *Journal of Petrology* **38**, 1585–1611.

Kay, R. W. (1978). Aleutian magnesian andesites-melts from subducted Pacific ocean crust. *Journal of Volcanology and Geothermal Resarch* **4**, 117–132.

Kay, R. W. & Kay, S. M. (1993). Delamination and delamination magmatism. *Tectonophysics* **219**, 177–189.

Kay, S. M., Ramos, V. A. & Marquez, M. (1993). Evidence in Cerro Pampa volcanic rocks of slab melting prior to ridge trench collision in southern South America. *Journal of Geology* **101**, 703–714.

Kepezhinskas, P. K., Defant, M. J. & Drummond, M. (1995). Na metasomatism in the island-arc mantle by slab melt–peridotite interaction: evidence from mantle interaction—evidence from mantle xenoliths in the north Kamchatka arc. *Journal of Petrology* **36**, 1505–1527.

Li, S., Xiao, Y., Liu, D., Chen, Y., Ge, N., Zhang, Z., *et al.* (1993). Collision of the North China and Yangtze Blocks and formation of coesite-bearing eclogites: timing and processes. *Chemical Geology* **109**, 89–111.

Li, X. H., Zhao, J. X., McCulloch, M. T., Zhou, G. Q. & Xing, F. M. (1997). Geochemical and Sm–Nd isotopic study of Neoproterozoic ophiolites from southeastern China: petrogenesis and tectonic implications. *Precambrian Research* **81**, 129–144.

Li, Z. X., Li, X. H., Zhou, H. & Kinny, P. D. (2002*a*). Grenvillian continental collision in South China: New SHRIMP U–Pb zircon results and implications for the configuration of Rodinia. *Geology* **29**, 211–214.

Li, X. H., Li, Z. X., Zhou, H. W., Liu, Y. & Kinny, P. D. (2002*b*). U–Pb zircon geochronology, geochemistry and Nd isotopic study of Neoproterozoic bimodal volcanic rocks in the Kangdian Rift of south China: implications for the initial rifting of Rodinia. *Precambrian Research* **113**, 135–154.

Li, X. H., Chen, Z. G., Liu, D. Y. & Li, W. X. (2003). Jurassic gabbro–granite–syenite suites from southern Jiangxi Province, SE China: age, origin and tectonic significance. *International Geological Review* **45**, 898–921.

Li, X. H., Chung, S. L., Zhou, H. W., Lo, C. H., Liu, Y. & Chen, C. H. (2004). Jurassic within-plate magmatism in southern Hunan–eastern Guangxi: $^{40}Ar/^{39}Ar$ dating, geochemistry, Sr–Nd isotopes, and implication for tectonic evolution of SE China. In: Malpas, J., Fletcher, C. & Ali, J. R. (eds) *Aspects of the Tectonic Evolution of China. Geological Society, London, Special Publications* **226**, 193–215.

Ludwig, K. R. (1999). Using Isoplot/EX, version 2, a geochronological toolkit for Microsoft Excel. Berkeley Geochronological Center Special Publication **1a**, 47.

Ludwig, K. R. (2001). Squid 1.02: a user manual. *Berkeley Geochronological Center Special Publication* **2**, 19.

Ma, C. Q., Yang, K. G. & Tang, Z. H. (1994). *Magma-Dynamics of Granitoids: Theory, Method and a Case Study of the Eastern Hubei Granitoids.* Wuhan: Publishing House of China University of Geosciences, pp. 1–260 (in Chinese with English abstract).

Mahoney, J. J., Frei, R., Tejada, M. L. G., Mo, X. X., Leat, P. T. & Nagler, T. P. (1998). Tracing the Indian Ocean mantle domain through time: isotopic results from old west Indian, east Tethyan, and South Pacific seafloor. *Journal of Petrology* **39**, 1285–1306.

Mao, J. W. & Wang, Z. L. (2000). A preliminary study on time limits and geodynamic setting of large-scale metallogeny in east China. *Mineral Deposits* **19**, 289–296 (in Chinese with English abstract).

Martin, H., Smithies, R. H., Rapp, R., Moyen, J. F. & Champion, D. (2005). An overview of adakite, tonalite–trondhjemite–granodiorite (TTG), and sanukitoid: relationships and some implications for crustal evolution. *Lithos* **79**, 1–24.

McInnes, B. I. A. & Cameron, E. M. (1994) Carbonated, alkaline hybridizing melts from a sub-arc environment: mantle wedge samples from the Tabar–Lihir–Tanga–Feni arc, Papua New Guinea. *Earth and Planetary Science Letters* **122**, 125–141.

Menzies, M. A., Long, A., Ingeram, G., Talnfl, M. & Janfcky, D. (1993). MORB periodotite–sea water interaction: experimental constrains on the behavior of trace elements, $^{87}Sr/^{86}Sr$ and $^{143}Nd/^{144}Nd$ ratios. In: Prichard, H. M., Alabaster, T., Harris, N. B. W. & Neary, C. R. (eds) *Magmatic Processes and Plate Tectonics. Geological Society, London, Special Publications* **76**, 309–322.

Muir, R. J., Weaver, S. D., Bradshaw, J. D., Eby, G. N. & Evans, J. A. (1995). Geochemistry of the Cretaceous Separation Point Batholith, New Zealand: granitoid magmas formed by melting of mafic lithosphere. *Journal of the Geological Society, London* **152**, 689–701.

Mungall, J. E. (2002) Roasting the mantle: slab melting and the genesis of major Au and Au-rich Cu deposits. *Geology* **30**, 915–918.

Oyarzún, R., Márquez, A., Lillo, J., López, I. & Rivera, S. (2001). Giant vs small porphyry copper deposits of Cenozoic age in northern Chile: adakitic vs normal calc-alkaline magmatism. *Mineralium Deposita* **36**, 794–798.

Pe-Piper, G. & Piper, J. W. (1994). Miocene magnesian andesites and dacites, Evia, Greece: adakites associated with subducting slab detachment and extension. *Lithos* **31**, 125–140.

Petford, N. & Atherton, M. (1996). Na-rich partial melts from newly underplated basaltic crust: the Cordillera Blanca Batholith, Peru. *Journal of Petrology* **37**, 1491–1521.

Polt, A. & Kerrich, R. (2002). Nd-isotope systematics of ~2·7 Ga adakites, magnesian andesites, and arc basalts, Superior Province: evidence for shallow crustal recycling at Archean subduction zones. *Earth and Planetary Science Letters* **202**, 345–360.

Prouteau, G., Scaillet, B., Pichavant, M., Pichavant, M. & Maury, R. C. (1999). Fluid-present melting of ocean crust in subduction zones. *Geology* **27**, 111–114.

Qu, X. M., Hou, Z. Q. & Li, Y. G. (2004). Melt components derived from a subducted slab in late orogenic ore-bearing porphyries in the Gangdese copper belt, southern Tibetan plateau. *Lithos* **74**, 131–148.

Rapp, R. P. & Watson, E. B. (1995). Dehydration melting of metabasalt at 8–32 kbar: implications for continental growth and crust–mantle recycling. *Journal of Petrology* **36**, 891–931.

Rapp, R. P., Watson, E. B. & Miller, C. F. (1991). Partial melting of amphibolite/eclogite and the origin of Archean trondhjemites and tonalites. *Precambrian Research* **51**, 1–25.

Rapp, R. P., Shimizu, N., Norman, M. D. & Applegate, G. S. (1999). Reaction between slab-derived melts and peridotite in the mantle wedge: experimental constraints at 3·8 GPa. *Chemical Geology* **160**, 335–356.

Rapp, R. P., Xiao, L. & Shimizu, N. (2002). Experimental constraints on the origin of potassium-rich adakite in east China. *Acta Petrologica Sinica* **18**, 293–311.

Rapp, R. P., Shimizu, N. & Norman, M. D. (2003). Growth of early continental crust by partial melting of eclogite. *Nature* **425**, 605–609.

Ratschbacher, L., Hacker, B. R., Webb, L. E., McWilliams, M., Ireland, T., Dong, S. W., *et al.* (2000). Exhumation of the ultrahigh-pressure continental crust in east central China: Cretaceous and Cenozoic unroofing and the Tan–Lu fault. *Journal of Geophysical Research* **105**, 13303–13338.

Richards, J. P. (2002). Discussion on 'Giant versus small porphyry copper deposits of Cenozoic age in northern Chile: Adakitic versus

normal calc-alkaline magmatism' by Oyarzun *et al.* (*Mineralium Deposita* **36**: 794–798, 2001). *Mineralium Deposita* **37**, 788–790.

Rui, Z. Y., Huang, C. K., Qi, G. M., Xu, J. & Zhang, H. T. (1984). *Porphyry Copper (Molybdenum) Deposits of China*. Beijing: Geological Publishing House, pp. 1–350 (in Chinese with English abstract).

Sajona, F. G., Naury, R. C., Pubellier, M., Leterrier, J., Bellon, H. & Cotton, J. (2000). Magmatic source enrichment by slab-derived melts in a young post-collision setting, central Mindanao (Philippines). *Lithos* **54**, 173–206.

Sen, C. & Dunn, T. (1994) Dehydration melting of a basaltic composition amphibolite at 1·5 and 2·0 GPa: implications for the origin of adakites. *Contributions to Mineralogy and Petrology* **117**, 394–409.

Sillitoe, R. H. (1997). Characteristic and controls of the largest porphyry copper–gold and epithermal gold deposits in the circum-Pacific region. *Australian Journal of Earth Sciences* **44**, 373–388.

Skjerlie, K. P. & Patiño Douce, A. E. (2002). The fluid-absent partial melting of a zoisite-bearing quartz eclogite from 1·0 to 3·2 GPa: implications for melting in thickened continental crust and for subduction-zone processes. *Journal of Petrology* **43**, 291–314.

Smith, R. E. & Smith, S. E. (1976). Comments on the use of Ti, Zr, Y, Sr, K, P and Na in classification of basaltic magmas. *Earth and Planetary Science Letters* **32**, 114–120.

Smithies, R. H. (2000). The Archean tonalite–trondhjemite–granodiorite (TTG) series is not an analogue of Cenozoic adakite. *Earth and Planetary Science Letters* **182**, 115–125.

Sorensen, S. S. & Grossman, J. N. (1989). Enrichment of trace elements in garnet amphibolites from a paleo-subduction zone: Catalina schist, southern California. *Geochimica et Cosmochimica Acta* **53**, 3155–3177.

Steiger, R. H. & Jager, E. (1977). Subcommission on geochronology: convention on the use of decay constants in geo- and cosmochronology. *Earth and Planetary Science Letters* **36**, 359–362.

Stern, C. R. & Kilian, R. (1996). Role of the subducted slab, mantle wedge and continental crust in the generation of adakites from the Austral Volcanic Zone. *Contributions to Mineralogy and Petrology* **123**, 263–281.

Sun, S. S. & McDonough, W. F. (1989). Chemical and isotopic systematics of oceanic basalts: implications for mantle composition and processes. In: Saunders, A. D. & Norry, M. J. (eds) *Implications for Mantle Composition and Processes, Magmatism in the Ocean Basins. Geological Society, London, Special Publications* **42**, 313–345.

Tang, Y. C., Xing, F. M., Wu, Y. C., Wang, Y. M., Chu, G. Z., Cao, F. Y., *et al.* (1998). *The Geology of Copper and Gold Polymetallic Deposits along the Yangtze River in Anhui Province*. Beijing: Geological Publishing House, pp. 1–349 (in Chinese with English abstract).

Thiéblemont, D., Stein, G. & Lescuyer, J. L. (1997). Epithermal and porphyry deposits: the adakite connection. *Comptes Rendus de l'Académie des Sciences* **325**, 103–109.

Tribuzio, R., Thirlwall, M. F., Vannucci, R. & Matthew, F. (2004). Origin of the gabbro–peridotite association from the Northern Apennine Ophiolites (Italy). *Journal of Petrology* **45**, 1109–1124.

Wang, Q. S. (1992). Research on the characteristics of the regional gravity field and geomagnetic field and crustal structure in Zhe–Wan area of Southeast China. In: Li, J. L. (ed) *Investigation on the Structure and Evolution of Oceanic and Continental Lithosphere in Southeast China*. Beijing: Chinese Science and Technology Publishing House, pp. 287–294 (in Chinese).

Wang, Q. (2000). *The Study Pertaining to Rock Probes of the Dynamics of the Deep Earth: Examples of Adakitic and Alkali-Rich Igneous Rocks in Southeast China (Including the Dabie Orogen)*. Postdoctoral research report of the Guangzhou Institute of Geochemistry, Chinese Academy of Sciences, pp. 69–108 (in Chinese with English abstract).

Wang, Q., Zhao, Z. H., Xu, J. F., Li, X. H., Bao, Z. W., Xiong X. L., *et al.* (2003*a*). Petrogenesis and metallogenesis of the Yanshanian adakite-like rocks in the Eastern Yangtze Block. *Science in China, Series D* **46**(supp.), 164–176.

Wang, Y. J., Fan, W. M., Guo, F., Pen, T. P. & Li, C. W. (2003*b*). Geochemistry of Mesozoic mafic rocks adjacent to Chenzhou–Linwu fault, South China: implications for the lithospheric boundary between the Yangtze and Cathaysia Blocks. *International Geology Review* **45**, 263–286.

Wang, Q., Xu, J. F., Zhao, Z. H., Xiong, X. L. & Bao, Z. W. (2003*c*). Petrogenesis of the Mesozoic intrusive rocks in the Tongling area, Anhui Province, China and their constraint to geodynamics process. *Science in China, Series D* **46**, 801–815.

Wang, Q., Xu, J. F., Zhao, Z. H., Bao, Z. W., Xu, W. & Xiong, X. L. (2004*a*). Cretaceous high-potassium intrusive rocks in the Yueshan–Hongzhen area of east China: adakites in an extensional tectonic regime within a continent. *Geochemical Journal* **38**, 417–434.

Wang, Q., Zhao, Z. H., Bao, Z W., Xu, J. F., Liu, W., Li, C. F., *et al.* (2004*b*). Geochemistry and petrogenesis of the Tongshankou and Yinzu adakitic intrusive rocks and the associated porphyry copper–molybdenum mineralization in southeast Hubei, east China. *Resource Geology* **54**, 137–152.

Wang, Y. J., Liao, C. L., Fan, W. M. & Peng, T. P. (2004*c*). Early Mesozoic OIB-type alkaline basalt in central Jiangxi Province and its tectonic implications. *Geochimica* **33**, 109–117 (in Chinese with English abstract).

Wang, Q., McDermott, F., Xu, J. F., Bellon, H. & Zhu, Y. T. (2005). Cenozoic K-rich adakitic volcanics in the Hohxil area, northern Tibet: lower crustal melting in an intracontinental setting. *Geology* **33**, 465–468.

Winchester, J. A. & Floyd, P. A. (1977). Geochemical discrimination of different magma series and their differentiation products using immobile elements. *Chemical Geology* **20**, 325–343.

Wyman, D. A., Ayer, J. A. & Devaney, J. R. (2000). Niobium-enriched basalts from the Wabigoon subprovince, Canada: evidence for adakitic metasomatism above an Archean subduction zone. *Earth and Planetary Science Letters* **179**, 21–30.

Xiong, X. L., Li, X. H., Xu, J. F., Li, W. X., Zhao Z. H., Wang, Q., *et al.* (2003). Extremely high-Na adakite-like magmas derived from alkali-rich basaltic underplate: the Late Cretaceous Zhantang andesites in the Huichang Basin, SE China. *Geochemical Journal* **37**, 233–252.

Xu, J. F. & Castillo, P. R. (2004). Geochemical and Nd–Pb isotopic characteristics of the Tethyan asthenosphere: implications for the origin of the Indian Ocean mantle domain. *Tectonophysics* **393**, 9–27.

Xu, X. S., Dong, C. W., Li, W. X. & Zhou, X. M. (1999). Late Mesozoic intrusive complexes in the coastal area of Fujian, SE China: the significance of the gabbro–diorite–granite association. *Lithos* **46**, 299–315.

Xu, J. F., Shinjio, R., Defant, M. J., Wang, Q. & Rapp, R. P. (2002) Origin of Mesozoic adakitic intrusive rocks in the Ningzhen area of east China: partial melting of delaminated lower continental crust? *Geology* **12**, 1111–1114.

Xu, J. F., Castillo, P. R., Chen, F. R., Niu, H. C., Yu, X. Y. & Zhen, Z. P. (2003). Geochemistry of late Paleozoic mafic igneous rocks from the Kuerti area, Xinjiang, northwest China: implications for backarc mantle evolution. *Chemical Geology* **193**, 137–154.

Zandt, G., Gilbert, H., Owens, T. J., Ducea, M., Saleeby, J. & Jones, C. H. (2004). Active foundering of a continental arc root beneath the southern Sierra Nevada in California. *Nature* **431**, 41–46.

Zhang, H. F., Sun, M. & Zhou, X. H. (2002). Mesozoic lithosphere destruction beneath the North China Craton: evidence from major- and trace-elements and Sr–Nd–Pb isotope studies of Fangcheng basalts. *Contributions to Mineralogy and Petrology* **144**, 241–253.

Zhang, Q., Qian, Q., Wang, E. C., Wang, Y., Zhao, T. P., Hao, J., *et al.* (2001). Existence of the East China Plateau in the mid–late Yanshan period: implications from adakites. *Scientia Geologica Sinica* **36**, 248–255 (in Chinese with English abstract).

Zhao, Z. H., Bao, Z. W., Zhang, B. Y. & Xiong, X. L. (2001). Crust–mantle interaction and its contribution to the Shizhuyuan super-large tungsten polymetallic mineralization. *Science in China, Series D* **31**, 266–276.

Zhou, J. X. (1999). *Geochemistry and Petrogenesis of Igneous Rocks Containing Amphibole and Mica: A Case Study of Plate Collision Involving Scotland and Himalayas*. New York and Beijing: Science Press, pp. 41–72.

Zhou, M. F., Yan, D. P., Kennedy, A. K., Li, Y. & Ding, J. (2002). SHRIMP U–Pb zircon geochronological and geochemical evidence for Neoproterozoic arc-magmatism along the western margin of the Yangtze Block, South China. *Earth and Planetary Science Letters* **196**, 51–67.

Zhou, X. M. & Li, W. X. (2000). Origin of Late Mesozoic igneous rocks in Southeast China: implications for lithosphere subduction and underplating of mafic magmas. *Tectonophysics* **326**, 269–287.

Zhou, X. M. & Zhu, Y. H. (1993). Late Proterozoic collisional orogen and geosuture in Southeastern China: petrological evidence. *Chinese Journal of Geochemistry* **12**, 239–251.

Zhu, J. C., Shen, W. Z., Liu, C. S. & Xu, S. J. (1990). Nd–Sr isotopic characteristics and petrogenesis discussion of Mesozoic granitoids in South China. *Acta Petrologica et Mineralogica* **9**, 97–104 (in Chinese with English abstract).

Zhu, X., Huang, C. K., Rui, Z. Y., Zhou, Y. H., Zhu, X. J., Hu, C. S., *et al.* (1983). *The Geology of the Dexing Porphyry Copper Ore Field*. Beijng: Geological Publications, pp. 1–336 (in Chinese with English abstract).